Elsevier Editorial System(tm) for BBA - Biomembranes

Manuscript Draft

Manuscript Number: BBAMEM-18-366R1

Title: Peptide antibiotic trichogin in model membranes: self-association and capture of fatty acids

Article Type: Regular Paper

Keywords: ESEEM; EPR; PELDOR; fatty acids; ion channels; trichogin

Corresponding Author: Professor Sergei Dzuba,

Corresponding Author's Institution: Russian Academy of Sciences

First Author: Ekaterina Afanasyeva

Order of Authors: Ekaterina Afanasyeva; Victoria Syryamina; Marta De Zotti; Fernando Formaggio; Claudio Toniolo; Sergei Dzuba

Abstract: The antimicrobial action of peptides in bacterial membranes is commonly related to their mode of self-assembling which results in pore formation. To optimize peptide antibiotic use for therapeutic purposes, a study on the concentration dependence of self-assembling process is thus desirable. In this work, we investigate this dependence for peptaibol trichogin GA IV (Tric) in the 1-palmitoyl-2-oleoyl-sn-glycero-3-phosphocholine (POPC) model membrane in the range of peptide concentrations between 0.5 and 3.3 mol %. Pulsed double electron-electron resonance (PELDOR) applied on spin-labeled peptide analogs highlights the onset of peptide dimerization above a critical peptide concentration value, namely ~ 2 mol %. Electron spin echo (ESE) envelope modulation (ESEEM) for D2O-hydrated bilayers shows that dimerization is accompanied by peptide re-orientation towards a trans-membrane disposition. For spin-labeled stearic acids (5-DSA) in POPC bilayers, the study of ESE decays and ESEEM in the presence of a deuterated peptide analog indicates that above the critical peptide concentration the 5-DSA molecules are attracted by peptide molecules, forming nanoclusters. As the 5-DSA molecules represent a model for the behavior of fatty acids participating in bacterial membrane homeostasis, such capturing action by Tric may represent an additional mechanism of its antibiotic activity.

Response to Reviewers: Response to Reviewers

Manuscript No.: BBAMEM-18-366
Title: Peptide antibiotic trichogin in model membranes: self-association and capture of fatty acids

Reviewer #1:
Comment: Highlights and Graphical Abstract are missing and should be added.
Response to comment: Done.

Comment: Carefully proofread/check the English, e.g.

P.3 last line "The lipids constituent the membrane are …": bad English

P.4 first line, "involved in various biochemical processes:" instead of "involved in various biochemical process:"
etc.
Response to comment: Done.

Reviewer #2:
Comment: Page 8, Results, first paragraph: “This effect, seen for the Tric1 concentration of 3.3 mol %, is large enough to be explained by a random distribution of spin labels…" It should be clarified why a large dipolar broadening has to be explained by a random distribution of spin labels. Pairs of spin labels with appropriate orientation and spin-spin distance distributions may also lead to such spectra. The difference in broadening observed for Tric1 and Tric8 indeed show that the spin labels are not distributed randomly, otherwise identical dipolar broadening would be expected for both samples.

Response to comment: We have rewritten this paragraph to clarify the situation – see the revised version with the changes marked.
Page 16, last paragraph: Eq. (4) has to be replaced by Eq. (5) at two places. Same in the Discussion, Capturing of fatty acids, first paragraph.
Response to comment: Done.

Reviewer #3:

Comment (i). CW EPR of Tric1 and Tric8: peptide self-association. The line-broadening in Fig. 1 at increasing peptide concentration is not so evidently clear for a BBA reader who is not specialist in this field. Then, once that peptide clusters formation is assumed, it is concluded that peptides self-associate through contacts in the N-terminal region.
Response to comment: We have rewritten description of Fig. 1 in the body text, to clarify the situation – see the revised version with the changes marked (Results, the first paragraph).

Comment (ii). PELDOR of Tric1 and Tric8: peptide dimerization. In contrast to what the authors state, the few data points reported in Fig. 3 do not suggest a saturation of the mean number of self-associated peptides and it is also difficult to understand the assumption of the presence of mixtures of monomers at low peptide concentration and dimers at high concentration.
Response to comment: We have changed (slightly) Fig. 3 to make our conclusions more convincing. Also, the description of this figure is amended – see 1st paragraph on P. 12.

Comment (iii). 2H ESEEM for Tric1 and Tric8 upon D2O-hydration: peptide location in the bilayers: whereas the dependence of the 2H-intensity in the frequency domain D2O-ESEEM spectra on the deuterons concentration and distance from the nitroxide moiety is not explained and for the ESEEM signals the reader is referred to Ref #14, assuming that the reader will be convinced that Tric1 is more inserted in the bilayer than Tric8, how can one be convinced from the data in Table 1 that a peptide reorientation does occur upon increasing concentrations?
Response to comment: We have rewritten 1st paragraph of this subsection to make it more clear.

Comment (iv). ESE decays for 5-DSA in presence of 'native' Tric: clustering of fatty acids. This is a paragraph on echo-detected spectra and anisotropic ESE-decays at two field positions of the spin-labeled stearic acid spectra that can be understood only by EPR specialists. Referring to references #14 and #31, from the time domain experiments, a biphasic dependence of spin-label surface concentration on Tric concentration is depicted in Fig. 5. How the data "unambiguously highlight" lateral cluster formation in the bilayers and, as the Tric concentration increases, the cluster are first destroyed and then become "larger and/or denser" is hard to understand. This sounds as a speculation.
Response to comment: We have added one sentence below Eq.(5) to clarify the situation.

Comment (v). ESEEM for 5-DSA in presence of DTric: peptide captures fatty acids. The experiments proved an interaction between the peptide and the fatty acids. The authors speculate on a clustering of fatty acids around the peptides related to their capture. Obtaining an estimate for a stoichiometric ratio would have been more desirable.

Response to comment: Unfortunately, it is impossible to derive the stoichiometric ratio from our data, because the cluster size seems to be too large to be detectable in these experiments. This interesting issue we discuss in more detail in the revised paper – see 2nd paragraph in the “Capturing of fatty acids“ subsection in the Discussion section.

Institute of Chemical Kinetics and Combustion

Russian Academy of Sciences, Siberian Branch

Ul. Institutskaya-3, Novosibirsk 630090, Russia

Prof. Sergei A. Dzuba
tel: +7 383 3331276
fax: +7 383 3307350
e-mail: dzuba@kinetics.nsc.ru

Dexember 5, 2018

Hans J. Vogel, Ph.D.

Executive Editor

BBA - Biomembranes

Dear Dr. Vogel,

We resubmit for publication in BBA Biomembranes the revised version of our paper “Peptide antibiotic trichogin in model membranes: self-association and capture of fatty acids”. We have found the comments of all 3 reviewers to be very valuable and amended the text accordingly.

With best regards,

Sergei A. Dzuba

Response to Reviewers

Manuscript No.: BBAMEM-18-366
Title: Peptide antibiotic trichogin in model membranes: self-association and capture of fatty acids

Reviewer #1:
Comment: Highlights and Graphical Abstract are missing and should be added.

Response to comment: Done.

Comment: Carefully proofread/check the English, e.g.

P.3 last line "The lipids constituent the membrane are …": bad English
P.4 first line, "involved in various biochemical processes:" instead of "involved in various biochemical process:"
etc.

Response to comment: Done.

Reviewer #2:

Comment: Page 8, Results, first paragraph: "This effect, seen for the Tric1 concentration of 3.3 mol %, is large enough to be explained by a random distribution of spin labels…" It should be clarified why a large dipolar broadening has to be explained by a random distribution of spin labels. Pairs of spin labels with appropriate orientation and spin-spin distance distributions may also lead to such spectra. The difference in broadening observed for Tric1 and Tric8 indeed show that the spin labels are not distributed randomly, otherwise identical dipolar broadening would be expected for both samples.

Response to comment: We have rewritten this paragraph to clarify the situation – see the revised version with the changes marked.

Page 16, last paragraph: Eq. (4) has to be replaced by Eq. (5) at two places. Same in the Discussion, Capturing of fatty acids, first paragraph.

Response to comment: Done.

Reviewer #3:

Comment (i). CW EPR of Tric1 and Tric8: peptide self-association. The line-broadening in Fig. 1 at increasing peptide concentration is not so evidently clear for a BBA reader who is not specialist in this field. Then, once that peptide clusters formation is assumed, it is concluded that peptides self-associate through contacts in the N-terminal region.

Response to comment: We have rewritten description of Fig. 1 in the body text, to clarify the situation – see the revised version with the changes marked (Results, the first paragraph).

Comment (ii). PELDOR of Tric1 and Tric8: peptide dimerization. In contrast to what the authors state, the few data points reported in Fig. 3 do not suggest a saturation of the mean number of self-associated peptides and it is also difficult to understand the assumption of the presence of mixtures of monomers at low peptide concentration and dimers at high concentration.

Response to comment: We have changed (slightly) Fig. 3 to make our conclusions more convincing. Also, the description of this figure is amended – see 1st paragraph on P. 12.

Comment (iii). 2H ESEEM for Tric1 and Tric8 upon D2O-hydration: peptide location in the bilayers: whereas the dependence of the 2H-intensity in the frequency domain D2O-ESEEM spectra on the deuterons concentration and distance from the nitroxide moiety is not explained and for the ESEEM signals the reader is referred to Ref #14, assuming that the reader will be convinced that Tric1 is more inserted in the bilayer than Tric8, how can one be convinced from the data in Table 1 that a peptide reorientation does occur upon increasing concentrations?

Response to comment: We have rewritten 1st paragraph of this subsection to make it more clear.

Comment (iv). ESE decays for 5-DSA in presence of 'native' Tric: clustering of fatty acids. This is a paragraph on echo-detected spectra and anisotropic ESE-decays at two field positions of the spin-labeled stearic acid spectra that can be understood only by EPR specialists. Referring to references #14 and #31, from the time domain experiments, a biphasic dependence of spin-label surface concentration on Tric concentration is depicted in Fig. 5. How the data "unambiguously highlight" lateral cluster formation in the bilayers and, as the Tric concentration increases, the cluster are first destroyed and then become "larger and/or denser" is hard to understand. This sounds as a speculation.

Response to comment: We have added one sentence below Eq.(5) to clarify the situation.

Comment (v). ESEEM for 5-DSA in presence of DTric: peptide captures fatty acids. The experiments proved an interaction between the peptide and the fatty acids. The authors speculate on a clustering of fatty acids around the peptides related to their capture. Obtaining an estimate for a stoichiometric ratio would have been more desirable.

Response to comment: Unfortunately, it is impossible to derive the stoichiometric ratio from our data, because the cluster size seems to be too large to be detectable in these experiments. This interesting issue we discuss in more detail in the revised paper – see 2nd paragraph in the "*Capturing of fatty acids*" subsection in the Discussion section.

*Graphical Abstract (for review)

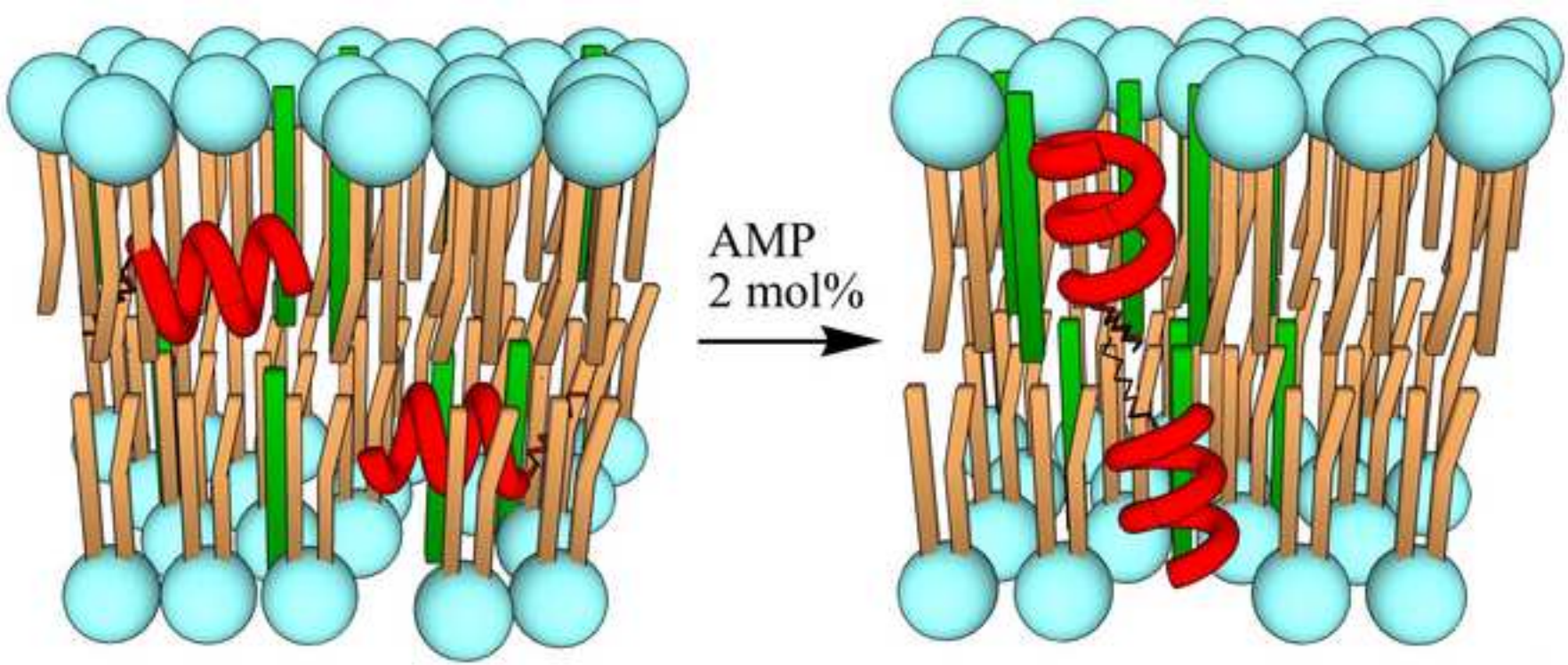

***Highlights (for review)**

- Antimicrobial peptide dimerization occurs above a critical concentration of 2 mol %
- Dimerization is accompanied by peptide *trans*-membrane re-orientation
- Free fatty acid in membranes are attracted by peptide molecules
- The attracted fatty acid molecules form nanoclusters around peptides

Peptide antibiotic trichogin in model membranes: self-association and capture of fatty acids

Ekaterina F. Afanasyeva,[a,b] Victoria N. Syryamina,[a,b] Marta De Zotti,[c] Fernando Formaggio,[c,d] Claudio Toniolo,[c,d] and Sergei A. Dzuba[a,b,*]

[a]Institute of Chemical Kinetics and Combustion, RAS, Novosibirsk 630090, Russian Federation

[b]Novosibirsk State University, Novosibirsk 630090, Russian Federation

[c]Department of Chemical Sciences, University of Padova, 35131 Padova, Italy

[d]Institute of Biomolecular Chemistry, Padova Unit, CNR, 35131 Padova, Italy

Abstract

The antimicrobial action of peptides in bacterial membranes is commonly related to their mode of self-assembling which results in pore formation. To optimize peptide antibiotic use for therapeutic purposes, a study on the concentration dependence of self-assembling process is thus desirable. In this work, we investigate this dependence for peptaibol trichogin GA IV (Tric) in the 1-palmitoyl-2-oleoyl-*sn*-glycero-3-phosphocholine (POPC) model membrane in the range of peptide concentrations between 0.5 and 3.3 mol %. Pulsed double electron-electron resonance (PELDOR) applied on spin-labeled peptide analogs highlights the onset of peptide dimerization above a critical peptide concentration value, namely ~ 2 mol %. Electron spin echo (ESE) envelope modulation (ESEEM) for D_2O-hydrated bilayers shows that dimerization is accompanied by peptide re-orientation towards a *trans*-membrane disposition. For spin-labeled stearic acids (5-DSA) in POPC bilayers, the study of ESE decays and ESEEM in the presence of a deuterated peptide analog indicates that above the critical peptide concentration the 5-DSA molecules are attracted by peptide molecules, forming nanoclusters. As the 5-DSA molecules represent a model for the behavior of fatty acids participating in bacterial membrane homeostasis, such capturing action by Tric may represent an additional mechanism of its antibiotic activity.

Keywords: dipolar spectroscopy, ESEEM, EPR, fatty acids, ion channels, PELDOR, trichogin

Introduction

The ever-increasing growth of antibiotic resistance in bacterial and fungal pathogens is a great challenge for modern medicine. Besides developing synthetic antibiotics of new generation, naturally-occurring antimicrobial agents and among them, antimicrobial peptides (AMPs) are generally considered as promising therapeutic agents [1]. Membrane-active peptides are a subclass of AMPs. They interact nonspecifically with bacterial membranes modifying their properties significantly, or even completely, retarding the onset of bacterial resistance. To optimize AMP design, a deep understanding of their mechanism of membrane destabilization would be extremely helpful.

The generally accepted mechanism for AMP membrane perturbation involves formation of channels or pores that increase ion and water flows through the lipid bilayer [2]. This phenomenon starts from peptide binding to lipid bilayer due to hydrophobic and electrostatic interactions. Then, peptides accumulate in the membrane and, after the peptide/lipid ratio attains a specific critical value, peptides self-associate in oligomers that eventually form channels. A precise knowledge of such critical peptide concentration value is highly desirable.

Besides, membrane perturbation processes may start at lower peptide concentration values. For example, at low concentrations peptides may still disrupt the local lipid chain packing and mobility [3]. A progressive membrane disordering was observed for different AMPs with increasing peptide concentration [4], and peptides were found able to enhance flip-flop lipid transitions between membrane leaflets and destroy cholesterol rafts in the membrane [5,6]. These perturbations influence the membrane thickness and flexibility [3,7-9].

Recently, we found peptide-induced redistribution of free fatty acids in the membrane mediated by the AMP alamethicin [10]. Free fatty acids are important components of

bacterial membranes because of their involvement in lipid homeostasis, protein functioning, signal transporting, and regulation functioning [11-13]. Therefore, redistribution of free fatty acids appears to be an alternative mechanism of peptide membrane-modifying action [10, 14].

Trichogin GA IV (Tric) is a natural undecapeptide (Scheme 1) isolated from the fungus *Trichoderma longibrachiatum*. Tric shows biological activity against Gram positive bacteria, has low hemolytic effect, and is stable to proteolysis [9,15,16]. 3D-Structural analysis indicated that Tric adopts a helical secondary structure [17-19], with a total peptide length of ~ 1.8-2.2 nm, that is about twice shorter than the lipid membrane thickness. A synthetic, covalent head-to-head Tric dimer exhibited a remarkably larger activity in comparison with the monomeric peptide [9]. Therefore, peptide self-assembling is required for pore formation by Tric.

Oligomerization of Tric results in transmembrane dimers [20,21]. Higher oligomers occur as well [22-25]. Tric self-association in the membrane is often accompanied by a change in peptide orientation from planar to transmembrane. However, for certain lipid compositions transmembrane oligomers are not formed even at high peptide concentrations [22, 26-28]. This phenomenon may be explained within the hypothesis of the carpet-like mechanism. Therefore, Tric membrane-perturbation mechanism is still under discussion.

Among other experimental techniques, pulsed EPR on spin-labeled molecules has proved to be a useful method to study peptide oligomerization and location in the membrane. Oligomerization may be investigated by pulsed electron-electron resonance [29], whereas location by electron spin echo (ESE) on deuterated systems using ESE envelope modulation method (^{2}H ESEEM) [20]. ESE decays can detect clusters of spin labels [10,30,31]. Conventional continuous wave (CW) EPR may provide complementary information as well.

Here, we employ CW and pulsed EPR techniques to study Tric, its partly deuterated analog ^{D}Tric, and the TOAC (1-oxyl-4-amino-2,2,6,6-tetramethylpiperidine-4-carboxylic acid) spin-labeled Tric analogs Tric^{1} and Tric^{8} (Scheme 1):

Scheme 1

*n*Oct-Aib-Gly-Leu-Aib-Gly-Gly-Leu-Aib-Gly-Ile-Leu-Lol (Tric)

*n*Oct(d_{15})-Aib-Gly-Leu(d_{10})-Aib-Gly-Gly-Leu(d_{10})-Aib-Gly-Ile(d_{10})-Lol (^{D}Tric)

*n*Oct-TOAC-Gly-Leu-Aib-Gly-Gly-Leu-Aib-Gly-Ile-Leu-Lol (Tric^{1})

nOct-Aib-Gly-Leu-Aib-Gly-Gly-Leu-TOAC-Gly-Ile-Leu-Lol (Tric^{8})

where *n*Oct is *n*-octanoyl, Aib is the non-proteinogenic α-aminoisobutyric acid, Lol is the 1,2-aminoalcohol leucinol and TOAC replaces Aib at either position 1 (Tric^{1}) or at position 8 (Tric^{8}). It is known that Aib→TOAC substitution does not alter the peptide membrane-modifying properties [27]. In the present study, all peptides are embedded in 1-palmitoyl-2-oleoyl-*sn*-glycero-3-phosphocholine (POPC) multilamellar vesicles.

Note that pulsed EPR studies on peptide location in model membranes was previously performed [20, 22] exploiting synthetic Tric analogs bearing the fluorescent, fluorenylmethyloxycarbonyl (Fmoc) group instead of the *n*Oct N$^{\alpha}$-blocking group [32].

In this work, we focus on two effects: (i) Tric self-assembling and (ii) Tric influence on the free fatty acid spatial distribution in POPC model membrane, using spin-labeled 5-doxyl-stearic acid (5-DSA) as a model for fatty acids.

Experimental

Sample preparation

The unlabeled peptide Tric and its partly deuterated analog ^{D}Tric were synthesized as described in [33, 34]. TOAC spin-labeled Tric analogs Tric^{1} and Tric^{8} were prepared by manual solid-phase peptide synthesis on a 2-chlorotrityl resin preloaded with Lol. The synthetic procedure followed for those two, new, TOAC-containing analogs closely resembles the one described in [35]. Tric^{1} and Tric^{8} were obtained in good yields (80% and 78%, respectively). The crude peptides were purified by medium-pressure liquid chromatography, by means of the Isolera Prime system Biotage (Sweden). POPC lipid was obtained from Avanti Polar Lipids (Birmingham, AL), 5-DSA was purchased from Sigma Aldrich (Germany). Methanol, ethanol and chloroform were Ekros-Analytica (St. Petersburg, Russia) products. A 10 mM phosphate buffered saline (PBS) containing 0.137 M NaCl and 0.0027 M KCl was used (pH = 7.0). In some cases, PBS was prepared with deuterated water. All commercial reagents were used without further purification.

Lipids, Tric analogs, and 5-DSA, taken at appropriate concentrations, were dissolved in chloroform. The solvent was slowly removed by nitrogen flow, followed by storage for 4 h *in vacuo* (10^{-2} bar). The dry lipid film was dispersed in buffer by vortex mixing. The amounts of buffer and lipid film were approximately the same (by weight). The sample was subjected to several cycles of rapid freezing-thawing. The large multilamellar vesicles (LMV) thus obtained [36] were kept at room temperature for 2 h and then transferred in a 5 mm o.d. tube (the sample length was about 5 mm), with 10% by weight dimethylsulfoxide added as a cryoprotector, and rapidly frozen in liquid nitrogen. The sample height did not exceed 5 mm.

EPR measurements

CW EPR experiments were carried out on an X-band Bruker ESP 380E EPR spectrometer using a dielectric Bruker ER 4118 X-MD-5 cavity and an Oxford Instruments CF-935 cryostat. The cryostat was cooled by nitrogen flow to 80 K. EPR spectra were

recorded at the modulation amplitude of 0.05 mT and modulation frequency of 100 kHz. The microwave power was set low enough to avoid spectra saturation.

All pulsed EPR experiments were carried out on an X-band Bruker ELEXSYS E580 EPR spectrometer equipped with a Bruker ER 4118 X-MD-5 cavity and an Oxford Instruments CF-935 cryostat. The cryostat was cooled by nitrogen flow to 80 K. Two-pulse echo decays, with the pulse sequence: $\pi/2$-τ-π-τ-*echo*, were obtained by scanning τ from 120 ns to 1.3 μs, with time steps of 4 ns. The ESE decay was measured at two different positions in the EPR spectra – at the maximum and the high-field shoulder of the echo-detected (ED) EPR spectra (see below). Three-pulse ESEEM experiments, with the pulse sequence: $\pi/2$-τ-$\pi/2$-T-$\pi/2$-τ-*echo*, were performed at the maximum of the ED-EPR spectra. The pulse lengths were 16 ns, τ was 204 ns, and the T interval was scanned from 248 ns to 10 μs with time steps of 12 ns. The data treatment was performed as described elsewhere [37]. A sixth-order polynomial fitting was applied to the relaxation decay in a semi-logarithmic plot. The modulus-Fourier transformation was performed on the normalized ESEEM decay using a MatLab home-made program.

Three-pulse PELDOR experiments were performed with the pulse sequence: $\pi/2_{(\nu A)}$-T-$\pi_{(\nu B)}$-(τ-T)-$\pi_{(\nu A)}$-τ-*echo*$_{(\nu A)}$, where the subscripts indicate two frequencies: one for detection (ν_A) and another for pumping (ν_B). The frequency offset ν_A-ν_B was 70 MHz, and ν_A and ν_B frequencies were chosen symmetrically around the center of the absorption dip in the resonator. The lengths of $\pi/2_{(\nu A)}$ and $\pi_{(\nu A)}$ pulses were 16 ns and 32 ns, respectively. The pumping pulse length was 32 ns. The amplitude of the $\pi_{(\nu B)}$ pulse was set to inverse the *echo*$_{(\nu A)}$ signal at the maximum of the echo-detected EPR spectra. The time τ was 800 ns. The time delay T for the pumping pulse was initially set to the negative value of -188 ns and then scanned with time intervals of 4 ns. The phase jumps due to the passage of the pumping $\pi_{(\nu B)}$

pulse through to the $\pi/2_{(vA)}$ pulse were eliminated by measuring the PELDOR decay for the samples without dipolar coupling [38].

Results

CW EPR of Tric[1] and Tric[8]: peptide self-association

Fig. 1 shows the CW EPR spectra recorded for the spin-labeled Tric[1] and Tric[8] at different peptide concentrations in POPC bilayers, at 80 K. One can see that an increase in peptide concentration results in line broadening, that clearly manifests itself in a relative decrease of the narrowest central component as compared with the wider low- and high-field components. For immobilized spin labels at low temperature, this broadening is induced by an electron-electron spin-spin dipole-dipole (d-d) interaction between spin labels [39]. The decrease of the central component seen for Tric[1] at a concentration of 3.3 mol % is larger than that seen for Tric[8] at a concentration of 5 mol %. This finding provides evidence that both peptides self-associate through contacts involving their N-terminal region.

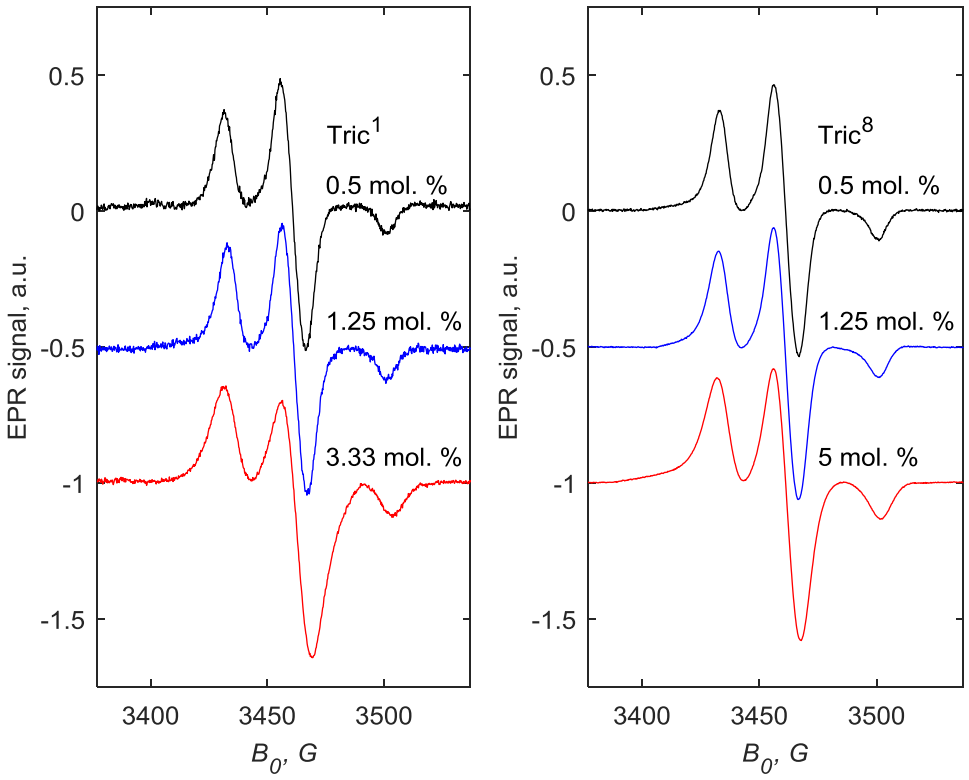

Fig. 1. CW EPR spectra of Tric[1] and Tric[8] in POPC bilayers taken at different peptide concentrations. Spectra are shifted along the vertical scale for convenience. Temperature: 80 K.

PELDOR of Tric[1] and Tric[8]: peptide dimerization

We obtained detailed information on spin label clustering using the PELDOR technique. PELDOR experiments with spin-labeled Tric analogs Tric[1] and Tric[8], were carried out at several peptide concentrations. The representative PELDOR signal dependences on the time delay *T* are shown in Fig. 2. Note that the large CW EPR line broadening observed for Tric[1] at 3.3 mol % concentration (Fig. 1) implies that in this case PELDOR data cannot be considered reliable, because of fast signal decay due to d-d interactions.

The PELDOR signal, *V*(*T*), is caused by d-d interactions between spin labels. For nanoscale clusters, these interactions are of two independent types, namely between

molecules associated in a cluster and between different clusters. Then, $V(T)$ may be presented as a product of two independent factors, $V_{INTRA}(T)$ and $V_{INTER}(T)$:

$$V(T) = V_{INTRA}(T) * V_{INTER}(T) \quad (1)$$

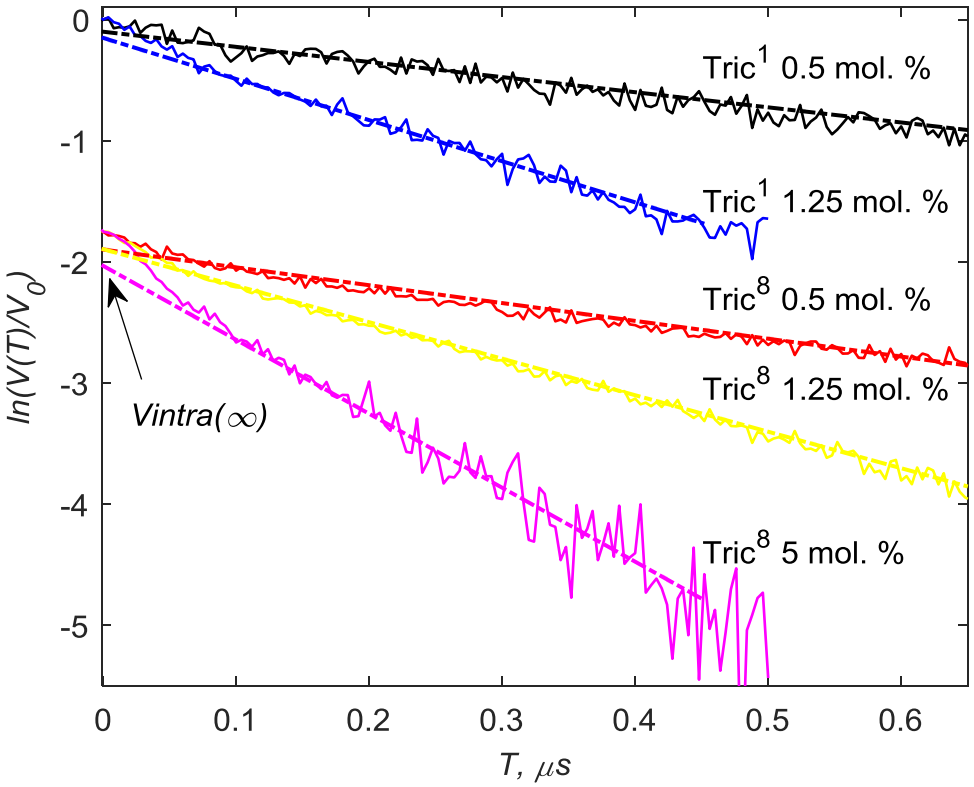

Fig. 2. Semi-logarithmic plot of representative PELDOR signal time dependences $V(T)$ at different peptide concentrations for Tric[1] and Tric[8]. Data for Tric[8] are shifted downwards for convenience. The dashed straight lines show linear asymptotes. Temperature: 80 K.

For a nanocluster formed by spin-labeled molecules, $V_{INTRA}(T)$ attains an asymptotic value [40]:

$$V_{INTRA}(\infty) = (1 - p_B)^{n-1}, \quad (2)$$

where p_B is the efficiency of the microwave excitation at the pumping frequency ν_B and n is the number of molecules in the cluster.

For a random spin-label distribution in the 3D-space, the $V_{INTER}(T)$ temporal dependence is a simple exponential:

$$V_{INTER}(T) = V_0 \exp\left(-\frac{4\pi^2}{9\sqrt{3}}\frac{g^2{\mu_B}^2}{\hbar}Cp_BT\right) \quad (3)$$

where g is the g-factor, μ_B is the Bohr magneton, C is the volume spin-label concentration (in cm^{-3}). Eq. (3) predicts that in the coordinates of Fig. 2 the $V(T)$ time dependence, after $V_{INTRA}(T)$ arrived to its asymptotic value, is expected to obey a linear dependence. This phenomenon is indeed observed (dashed lines in this plot).

From extrapolation of the dashed lines in Fig. 2 the $V_{INTRA}(\infty)$ value can be obtained. In turn, it provides the mean number n in a cluster by use of Eq. (2), if p_B is known. This latter value is calculated by taking into account the overlapping of excitation bandwidths for the A and B spins [41]:

$$p_B = \frac{p_B^0}{1 - p_A^0}$$

where

$$p_{B(A)}^0 = \int_0^\infty \frac{\omega_1^2}{\omega_1^2 + (\omega - \omega_{B(A)})^2} \sin^2\left(\frac{t_p}{2}\sqrt{\omega_1^2 + (\omega - \omega_{B(A)})^2}\right) A(\omega) d\omega \approx 2\omega_1 A(\omega_{B(A)}) \quad (4)$$

where $A(\omega)$ is a function describing the spin-label EPR absorptive lineshape (with the integral normalized to unity), $\omega_{B(A)} = 2\pi\nu_{B(A)}$, ω_1 is the microwave amplitude, and t_p is the pumping pulse length; the given approximate estimation for $p_{B(A)}^0$ is valid for $\omega_1 t_p = \pi$ and ω_1 smaller than spectral linewidth. Previously [14], it was shown that this approach provides good agreement with experiment.

Employing the obtained data on $V_{INTRA}(\infty)$ values and Eq. (2), the *n* values were found. As these values were not integer numbers, a mixture of monomers and dimers should be assumed to be present in the samples. So, instead of *n*, it would be more reasonable to use a mean number <*n*>. The results of <*n*> calculations are shown in Fig. 3. One can see that at small peptide concentrations the dependence is linear (and similar for both Tric[1] and Tric[8] analogs), while a saturated-like behavior is observed at higher concentrations. A tenfold increase in peptide concentration (from 0.5 to 5 mol %) results in the <*n*> value rising from 1.15 ± 0.03 (at 0.5 mol %) to 1.90 ± 0.07 (at 5 mol %). Such findings prove that at low concentrations mostly peptide monomers are present while at high concentrations dimers are prevailing.

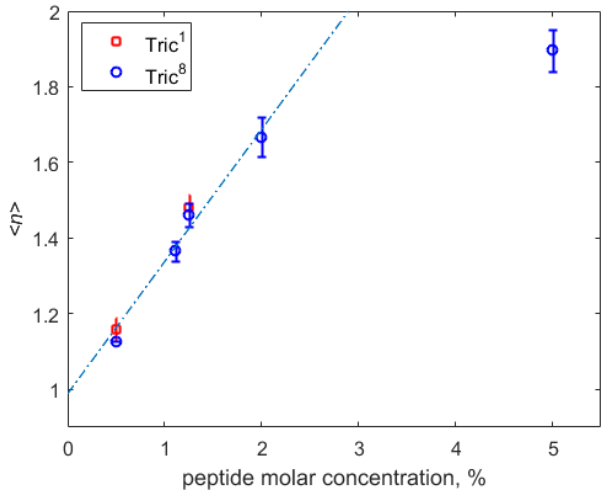

Fig. 3. Mean number <*n*> of self-associated peptide molecules obtained using Eq. (2) from the PELDOR data (shown in Fig. 2). The straight dash-dotted line indicates a linear dependence at low concentrations.

^{2}H ESEEM for Tric^1 and Tric^8 upon D_2O-hydration: peptide location in the bilayer

Information on the location of spin-labeled peptides in the membrane can be obtained from ESEEM experiments on D_2O-hydrated bilayers [14, 20, 37]. The ^{2}H ESEEM signal in this approach depends on the distance between the spin label and the deuterium nuclei [42].

So the closer the spin label is to the membrane surface, the larger the ^{2}H ESEEM line intensity is expected. The measurements performed in this work for Tric^1 and Tric^8 resulted in frequency-domain ESEEM spectra looking similar to those presented in [14]. The spectra show a narrow line positioned at 2.2 MHz, that is the deuterium Larmor frequency (at the microwave X-band). The experimentally obtained intensities for the narrow line A_N (see definition in [14], Fig. 6 therein) at low, ~ 0.5 mol %, and large, ~ 5 mol %, peptide concentrations are given in Table 1. Literature data [20-22] for closely-related, spin-labeled Tric analogs in membrane bilayers of different lipid compositions are also reported in Table 1 for comparison. Note that the spin-labeled Tric analogs studied in the cited papers [and herein termed: Fmoc-Tric^1-OMe and Fmoc-Tric^8-OMe (OMe, methoxy)] carried an N-terminal Fmoc- instead of the native *n*Oct- group, and a leucine methyl ester at their C-terminus (instead of the naturally-occurring 1,2-aminoalcohol Lol).

Table 1. Intensity of the ^{2}H ESEEM line at the deuterium Larmor frequency, A_N/MHz^{-1}, for Tric^1 and Tric^8 peptide analogs in D_2O-hydrated bilayers at two peptide concentrations

Peptide / Bilayer	Tric^1, 0.5 mol %	Tric^1, 5 mol %	Tric^8, 0.5 mol %	Tric^8, 5 mol %	Reference
POPC	**0.036**	**0.031**	**0.020**	**0.027**	**This work**
POPC	0.086	0.0515	0.052	0.047	[21]*
ePC**/cholesterol	0.12	0.05	0.12	0.12	[22]*
DPPC**	0.10	0.05	0.07	0.05	[20]*,***

The experimental uncertainty is not larger than 10 %.

*These data refer to the two Tric analogs Fmoc-Tric^1-OMe and Fmoc-Tric^8-OMe.

**ePC is egg phosphatidylcholine and DPPC is 1,2-dipalmitoyl-sn-glycero-3-phosphocholine.

***A_N in arbitrary units.

Data in Table 1 show that substitution of *n*Oct by Fmoc results in larger A_N values. This finding implies that Fmoc-Tric^1-OMe and Fmoc-Tric^8-OMe are located closer to the bilayer surface than Tric^1 and Tric^8. For Tric^1, A_N decreases by a factor of 1.16 with increasing concentration, while for Tric^8 it increases by a factor of 1.35. This means that, while the peptide concentration increases, the label at position 1 becomes more inserted into the membrane while that at position 8 becomes closer to the membrane surface. Both findings point towards a peptide reorientation upon increasing concentration.

This behavior is to be compared with that of Fmoc-Tric^1-OMe and Fmoc-Tric^8-OMe in different lipid bilayers, where (as the peptide concentration increases) a greater decrease in A_N value is registered for the spin-label at position 1 under all experimental conditions

(decrease factors from 1.7 to 2.2), while for the spin label at position 8 unchanged or slightly lower A_N values (decrease factor of ~ 1.3) are registered.

In conclusion, an increase in peptide concentration results in (i) a deeper insertion in the lipid bilayer of the N-terminal part of the peptide for Fmoc-containing analogs than *n*Oct-containing ones (that are less deeply inserted). (ii) The peptide C-terminus is somewhat exposed on the bilayer surface for *n*Oct-containing analogs, while slightly buried into it for Fmoc-containing ones.

ESE decays for 5-DSA in presence of 'native' Tric: clustering of fatty acids

CW EPR spectra recorded for 5-DSA in POPC bilayers showed the typical lineshape for immobilized nitroxide spin labels. Upon (*unlabelled*) Tric addition, the EPR spectra did not change noticeably, showing only a slight line broadening in response to increasing peptide concentration, as a result of dipole-dipole (d-d) interactions (similar to those published in [31]). Thus, we decided to apply ESE to study d-d interactions between 5-DSA molecules, since ESE decays are known to be much more sensitive to d-d interactions than CW EPR spectra.

In the nanoscale range of distances, d-d interactions between spin labels can be readily detected by measuring the "instantaneous spectral diffusion" effect [31] in ESE decays. This effect takes place because the microwave pulses "instantly" flip the magnetic dipolar field (acting on the selected spin by a coupled spin). This effect results in an additional defocusing of the ESE signal. (Note that PELDOR spectroscopy is based on the same physical principle, but the flip of the magnetic dipolar field is performed applying pulses at different microwave frequencies). ESE decays are sensitive to nanoscale local concentrations because d-d interactions matter up to distances *r* (determined by the relation $r \sim \sqrt[3]{\gamma^2 \hbar \tau}$) of about 10 nm, as in organic solids τ is typically in the μs time range.

In the case of a random 3D-space distribution, this mechanism results in the same analytical formula as Eq. (3), with time T replaced by 2τ, $\omega_A = \omega_B$ (the excitation and detection frequencies are the same), and $p_A^0 = 0$. Spin labels in 5-DSA molecules embedded into membranes are expected to exhibit a 2D-space distribution (in the case of Tric[1] and Tric[8], the spin label locations may remarkably deviate from the in-plane position, so that in this case a 3D-distribution is preferable). Instead of Eq. (3), the ESE decays for a 2D-distribution are described fairly well by the approximated formula [31]:

$$E_{2D}(\tau) \cong E_0 \exp\{-3.21\sigma p_B (g^2\mu_B^2\tau/\hbar)^{\frac{2}{3}}\} \quad (5)$$

where σ is the spin label surface concentration measured in cm^{-2} units. Therefore, we can obtain the local surface concentration σ of spin-labeled molecules directly from the ESE decays, by plotting $\ln(E_{2D}(\tau))$ as a function of $\tau^{\frac{2}{3}}$.

However, the ESE signal decays through many different relaxation mechanisms. To refine the pure contribution of the instantaneous diffusion effect, one should perform measurements with different p_B values, because at cryogenic temperatures the other relaxation mechanisms are expected to be independent of this parameter. From Eq. (4), it follows that this study can be carried out by measuring ESE decays at two different spectral positions. For ESE decays obtained at two field positions and divided by each other, the p_B parameter in Eq. (5) should be replaced by the difference $[p_B(1) - p_B(2)]$, where numbers in parenthesis denote the two field positions.

Fig. 4 shows the ratio between echo time traces obtained at the two field positions (indicated by arrows in the figure inset). Data are given for 5-DSA at 1 mol. % concentration in the POPC bilayer, as a function of increasing Tric concentration (from 0 to 3.3 mol %). The coordinates employed are convenient for comparison with Eq. (5). The small oscillations

seen in the curves are ESEEM induced by electron-nuclear interactions with the neighboring proton spins. Fig. 4 shows that the echo decays obey the $\tau^{\frac{2}{3}}$ time dependence predicted by Eq. (5).

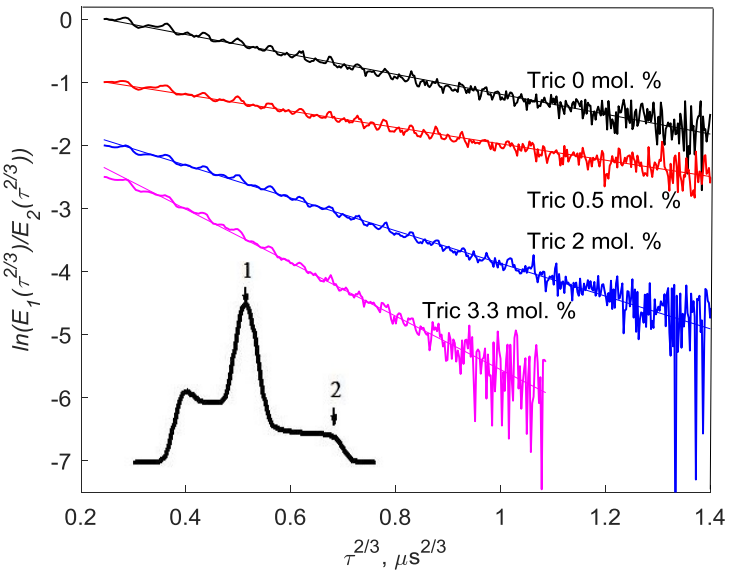

Fig. 4. Ratio between ESE time traces taken for 5-DSA in POPC bilayers at two field positions in the EPR spectrum (as indicated by arrows in the inset) at different Tric concentrations. Data are plotted in the coordinates suitable for comparison with Eq. (5). Curves are shifted along the vertical axis for convenience. The 5-DSA concentration is 1 mol %. Measurements were performed at 80 K.

ESE decays in Fig. 4 depend remarkably on Tric concentration. To employ the theoretical Eq. (5), the parameter $[p_B\,(1) - p_B\,(2)]$ must be determined. This calculation was carried out as described in [14]. The value found for this parameter is 0.19 ± 0.02. Then, applying Eq. (5) to the linear dependences in Fig. 4, we obtained the surface densities σ. These data are plotted in Fig. 5 as a function of Tric concentration, in dimensionless units by dividing σ by the host lipid lateral density in the bilayer, σ_0. The latter parameter was

estimated to be $\sigma_0 \approx 1.7\,10^{14}$ cm^{-2} (see [31] for details), that corresponds to the mean area per lipid ~ 0.60 nm^2.

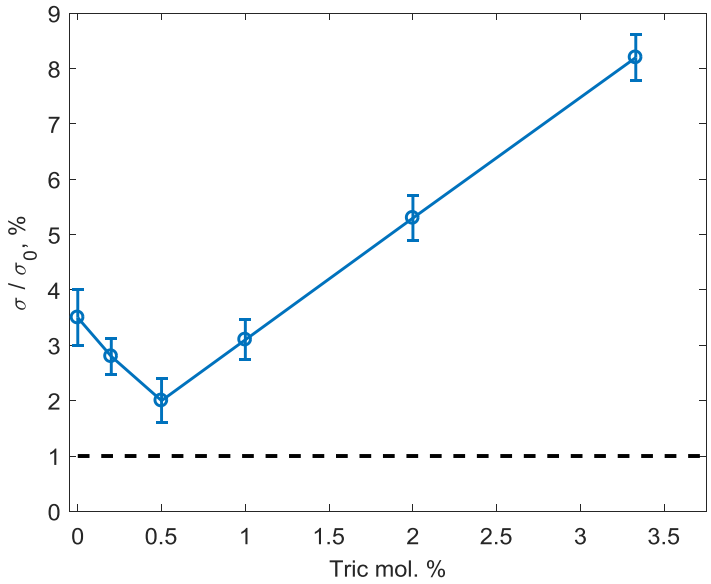

Fig. 5. 5-DSA surface concentration σ in the presence of Tric in POPC bilayers, as a function of increasing peptide concentration, as obtained from the slopes reported in Fig. 4. The solid lines are drawn to guide the eye. The mean 5-DSA concentration (1 mol %) in the bilayer is indicated by the horizontal dashed line.

Data in Fig. 5 clearly indicate that the σ value largely exceeds the mean free fatty acid concentration (1 mol %) in the bilayer. This enhancement unambiguously highlights that 5-DSA molecules form lateral clusters in the bilayer. These clusters are formed even in the absence of Tric. This finding is in agreement with our previous data [10, 31]. Fig. 5 shows that, as the Tric concentration increases, clusters are first destroyed (this effect is however small) and then, with a further peptide concentration increase (above 1 mol %), the clusters becomes larger and/or denser. One may conclude therefore that peptide promotes cluster formation.

ESEEM for 5-DSA in presence of ^{D}Tric: peptide captures fatty acids

We suggest that the experimentally found noticeable increase of the local 5-DSA concentration in the bilayer in the presence of Tric is essentially the result of a mutual attraction between fatty acids and Tric molecules, with formation of a 5-DSA nanocluster around the peptide. To support this hypothesis, ESEEM experiments were performed for 5-DSA with the deuterated peptide ^{D}Tric (Scheme 1). The ^{2}H-ESEEM effect is known to be detected when the unpaired electron of a spin label and the deuterium nucleus are separated by a distance no longer than 0.8 - 1 nm [43]. Clearly, this experiment can provide a good evidence for a close contact between 5-DSA and Tric molecules.

The ^{2}H ESEEM data obtained for 5-DSA in POPC bilayer at different ^{D}Tric peptide concentrations are reported in Fig. 6. The ESEEM spectra in the frequency domain show a narrow line positioned at 2.2 MHz (Fig. 6, left) assigned to the deuterium Larmor frequency (at the X-band). Data in Fig. 6 (right) show that A_N increases with increasing peptide concentration until 2 mol % peptide concentration. Then, a plateau is reached at larger peptide concentrations.

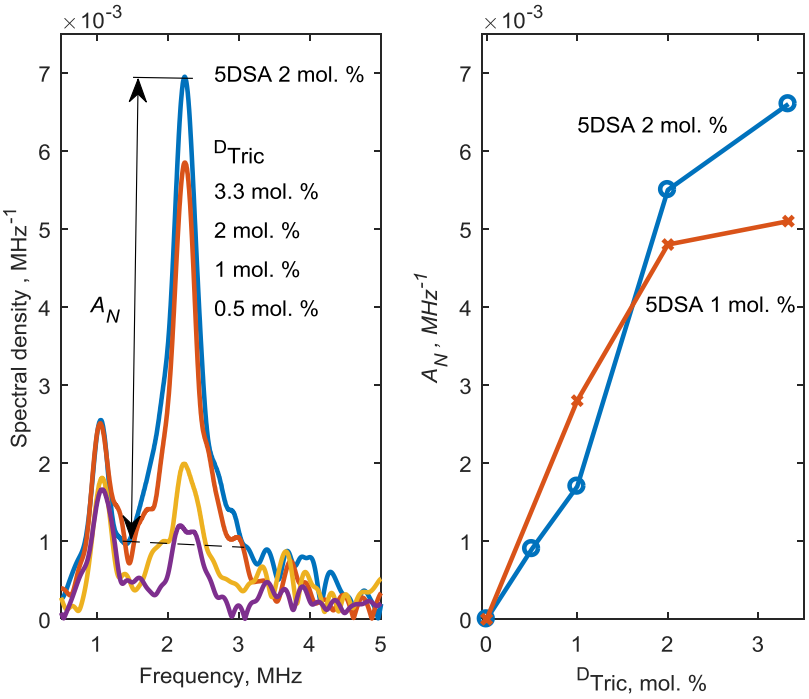

Fig. 6. Left: ^{2}H ESEEM spectra for 5-DSA in POPC bilayers at different ^{D}Tric concentrations. Right: the 2.2 MHz line intensity as a function of ^{D}Tric concentration, at 1 mol% and 2 mol % 5-DSA concentrations.

For the putative case of a random 5-DSA spatial distribution in the membrane, one can estimate that for 1 mol % 5-DSA concentration the mean distance between molecules is around ~ 7 nm. This value is significantly larger than that of 1 nm [43] which represents the upper boundary for the onset of the ^{2}H ESEEM effect. Therefore, the effect presented in Fig. 6 unambiguously proves that peptides capture fatty acids. Taking into account the data described above on the ESE decays for 5-DSA in the presence of *unlabelled* Tric, this capture results in a clustering of the 5-DSA molecules around the peptides.

Discussion

Peptide dimerization and location

PELDOR data in Figs. 2 and 3 clearly demonstrate that peptides form dimers. CW EPR data in Fig. 1 show that dimerization occurs through interaction of two N-termini (head-to-head dimerization). This result is in agreement with previous PELDOR data on the Fmoc-Tric^{1}-OMe and Fmoc-Tric^{8}-OMe peptide analogs [20,21] where the authors reported n = 2.1 ± 0.1 at 5 mol % peptide concentration [20]. These dimers possibly induce membrane leakage [21].

The dependence of the mean number $<n>$ of peptide molecules in the self-associated species on peptide concentration seen in Fig. 3 may be interpreted with the onset of an equilibrium between peptide monomers and dimers in the membrane. The critical peptide concentration value where dimers become dominating is ~ 2 mol %.

ESEEM data on D_2O-hydrated bilayers (Table 1) demonstrate that Tric^{1} and Tric^{8} molecules are located deeper in the membrane core than Fmoc-Tric^{1}-OMe and Fmoc-Tric^{8}-OMe analogs (the A_N values in the former case are smaller). We explain this difference by noting that the bulkier and more rigid Fmoc- group in the latter analogs may reasonably cause a deeper peptide insertion into the membrane core. Data in Table 1 also show that as concentration increases, peptide molecules change their orientation in the membrane, with the N-terminus going deeper into the membrane interior and the C-terminus moving closer to the membrane surface. Note that a slight tendency for *n*Oct-Tric^{1}-OMe inserting in the membrane core and for *n*Oct-Tric^{8}-OMe moving to the membrane surface was also observed in [32].

Capturing of fatty acids

Fig. 4 shows that d-d-induced ESE decays for 5-DSA molecules obey the theoretical expression (5) which predicts a proportionality to $(\gamma^2 \hbar\, \tau)^{2/3}$. This behavior means that the spin labels in the 5-DSA molecules possess a 2D-distribution, as one may naturally expect for a

bilayer. Eq. (5) allows one to directly obtain the surface density σ. The calculated σ values deviate from those expected for homogeneously distributed molecules (Fig. 5). This effect, previously reported for POPC bilayers [10, 31], and DPPC and DOPC (1,2-dioleoyl-*sn*-glycero-3-phosphocholine) bilayers [31], is interpreted by formation of 5-DSA molecular nanoclusters. The 5-DSA local concentration in such clusters increases with increasing peptide concentration. The results in Fig. 5 indicate that peptides promote cluster formation.

This phenomenon is confirmed by ^{2}H ESEEM experiments on 5-DSA in the presence of ^{D}Tric (Fig. 6), where A_N is seen to strongly increase with increasing 5-DSA concentration (with saturation occurring above 2 mol %). Thus, one may conclude that 5-DSA clusters are formed around the peptide molecules. By comparison with the results of a previous computer modelling study [31] we can state that the size of such clusters is larger than 20 nm (below this value, the time traces in Fig. 4 are expected to become stretched – see Fig. 1 in [31]).

It is interesting to note that this nanocluster formation around peptide molecules occurs in the same concentration range where dimers are formed, namely around a peptide concentration of ~ 2 mol % (Fig. 3). Probably, peptide dimers disrupt the neighbor lipid packing and stearic acid molecules compensate for this perturbation.

Free fatty acids are building blocks for lipids and a component of bacterial membranes that regulates its physical properties such as a fluidity and rigidity [44]. Fatty acids also facilitate peptide/protein "anchoring" and traffic along the membrane by palmitoylation, a type of covalent attachment of free fatty acids to specific amino acids [45], that is relevant for peptide and protein functioning [11-13,45], and participate in signal transporting and regulation functioning [46, 47]. In summary, redistribution of free fatty acids seems to be an alternative mechanism by which peptides exert their membrane-modifying action [10,14].

Conclusion

In this work we studied two effects by which peptide antibiotic Tric perturbs the lipid membrane. The first effect involves peptide self-assembling to dimers which may induce membrane leakage. In the second, capture of free fatty acids by peptide molecules takes place in the bilayer, possibly leading to a disturbance of lipid homeostasis in the bacterial membrane. Both processes become effective above a critical peptide concentration, found to be around 2 mol % for Tric.

Below that critical concentration, the peptide molecules occur in the monomeric state in the membrane and free fatty acids form local clusters. At low peptide concentrations, both fatty acid clusters and peptides exist independently. Above the critical peptide concentration, Tric tends to form dimers, while clusters of fatty acids become denser, with a simultaneous mutual attraction between fatty acid clusters and peptides taking place. As free fatty acids are involved in membrane functioning, this capturing effect may perturb the physiological functions of the membrane and thus play an important role in peptide antibiotic action.

Acknowledgements

This work was supported by the Russian Science Foundation, project No. 15-15-00021. VNS is grateful to the Russian Foundation for Basic Research for its support with project # 17-44-543240. MDZ and FF gratefully acknowledge MIUR for financial support (FIRB 2013: project No. RBFR13RQXM and PRIN 2015: project No. 20157WW5EH).

References

[1] (a) K.A. Brogden, Antimicrobial peptides: pore formers or metabolic inhibitors in bacteria? Nature Rev. Microbiol. 3 (2005) 238-250; (b) K.V.R. Reddy, R.D. Yedery, C. Aranha, Antimicrobial peptides: premises and promises, Int. J. Antimicrob. Agents 24 (2004) 536-547.

[2] (a) M.S. Sansom, Alamethicin and related peptaibols: model ion channels, Eur. Biophys. J. 22 (1993) 105-124. (b) P. Tieleman, J. Bentz, Molecular dynamics simulation of the evolution of hydrophobic defects in one monolayer of a phosphatidylcholine bilayer: relevance for membrane fusion mechanisms, Biophys. J. 83 (2002) 1501-1510. (c) O.S. Andersen, R.E. Koeppe, B. Roux, Gramicidin channels, IEEE, Trans. Nanobiosci. 4 (2005) 10-20.

[3] A.J. Costa-Filho, Y. Shimoyama, J.H. Freed, A 2D-ELDOR study of the liquid ordered phase in multilamellar vesicle membranes, Biophys. J. 84 (2003) 2619-2633.

[4] M. Bortolus, A. Dalzini, C. Toniolo, K.-S. Hahm, A.L. Maniero, Interaction of hydrophobic and amphipathic antimicrobial peptides with lipid bicelles, J. Pept. Sci. 20 (2014) 517-525.

[5] S. Qian, W.T. Heller, Peptide-induced asymmetric distribution of charged lipids in a vesicle bilayer revealed by small-angle neutron scattering, J. Phys. Chem. B 115 (2011) 9831-9837.

[6] S. Qian, D. Rai, W.T. Heller, Alamethicin disrupts the cholesterol distribution in dimyristoyl phosphatidylcholine–cholesterol lipid bilayers, J. Phys. Chem. B 118 (2014) 11200-11208.

[7] L.I. Horvath, P.J. Brophy, D. Marsh, Exchange rates at the lipid-protein interface of myelin proteolipid protein studied by spin-label electron spin resonance, Biochemistry 27 (1988) 46-52.

[8] B. Bechinger, The structure, dynamics and orientation of antimicrobial peptides in membranes by multidimensional solid-state NMR spectroscopy, Biochim. Biophys. Acta - Biomembr. 1462 (1999) 157-183.

[9] C. Toniolo M. Crisma, F. Formaggio, C. Peggion, V. Monaco, C. Goulard, S. Rebuffat, B. Bodo, Effect of N^{α}-acyl chain length on the membrane-modifying properties of synthetic analogs of the lipopeptaibol trichogin GA IV, J. Am. Chem. Soc. 118 (1996) 4952-4958.

[10] E. F. Afanasyeva, V. N. Syryamina, S. A. Dzuba, Communication: Alamethicin can capture lipid-like molecules in the membrane, J. Chem. Phys. 146 (2017) 011103/1-4.

[11] D.D. Martin, E. Beauchamp, L.G. Berthiaume, Post-translational myristoylation: fat matters in cellular life and death, Biochimie 93 (2011) 18-31.

[12] Y.-M. Zhang, C.O. Rock, Membrane lipid homeostasis in bacteria, Nat. Rev. Microbiol. 6 (2008) 222-233.

[13] A.W. Smith, Lipid-protein interactions in biological membranes: a dynamic perspective Biochim. Biophys. Acta - Biomembr. 1818 (2012) 172-177.

[14] V.N. Syryamina, M. De Zotti, C. Toniolo, F. Formaggio, S.A. Dzuba, Alamethicin self-assembling in lipid membranes: concentration dependence from pulsed EPR of spin labels, Phys. Chem. Chem. Phys. 20 (2018) 3592-3601.

[15] M. De Zotti, B. Biondi, F. Formaggio, C. Toniolo, L. Stella, Y. Park, K.-S. Hahm, Trichogin GA IV: an antibacterial and protease-resistant peptide, J. Pept. Sci. 15 (2009) 615-619.

[16] M. De Zotti, B. Biondi, Y. Park, K.-S. Hahm, M. Crisma, C. Toniolo, F. Formaggio, Antimicrobial lipopeptaibol trichogin GA IV: role of the three Aib residues on conformation and bioactivity, Amino Acids 43 (2012) 1761-1777.

[17] C. Toniolo, C. Peggion, M. Crisma, F. Formaggio, X. Shui, D. S. Eggleston, Structure determination of racemic trichogin A IV using centrosymmetric crystals, Nat. Struct. Mol. Biol. 1 (1994) 908-914.

[18] D. J. Anderson, P. Hanson, J. Mc Nulty, G. L. Millhauser, V. Monaco, F. Formaggio, M. Crisma, C. Toniolo, Solution structures of TOAC-labeled trichogin GA IV peptides from allowed ($g \approx 2$) and half-field electron spin resonance, J. Am. Chem. Soc. 121 (1999) 6919-6927.

[19] A. D. Milov, A. G. Maryasov, Yu. D. Tsvetkov, J. Raap, Pulsed ELDOR in spin-labeled polypeptides, Chem. Phys. Lett. 303 (1999) 135-143.

[20] E. S. Salnikov, D. A. Erilov, A. D. Milov, Yu. D. Tsvetkov, C. Peggion, F. Formaggio, C. Toniolo, J. Raap, S. A. Dzuba, Location and aggregation of the spin-labeled peptide trichogin GA IV in a phospholipid membrane as revealed by pulsed EPR, Biophys. J. 91 (2006) 1532-1540.

[21] V. N. Syryamina, N. P. Isaev, C. Peggion, F. Formaggio, C. Toniolo, J. Raap, S. A. Dzuba, Small-amplitude backbone motions of the spin-labeled lipopeptide trichogin GA IV in a lipid membrane as revealed by electron spin echo, J. Phys. Chem. B 114 (2010) 12277-12283.

[22] V. N. Syryamina, M. De Zotti, C. Peggion, F. Formaggio, C. Toniolo, J. Raap, S. A. Dzuba, A molecular view on the role of cholesterol upon membrane insertion, aggregation, and water accessibility of the antibiotic lipopeptide trichogin GA IV as revealed by EPR, J. Phys. Chem. B 116 (2012) 5653-5660.

[23] M. Smetanin, S. Sek, F. Maran, J. Lipkowski, Molecular resolution visualization of a pore formed by trichogin, an antimicrobial peptide, in a phospholipid matrix, Biochim. Biophys. Acta – Biomembr. 1838 (2014) 3130-3136.

[24] T. N. Kropacheva, J. Raap, Voltage-dependent interaction of the peptaibol antibiotic zervamicin II with phospholipid vesicles, FEBS Lett. 460 (1999) 500-504.

[25] L. Stella, C. Mazzuca, M. Venanzi, A. Palleschi, M. Didonè, F. Formaggio, C. Toniolo, B. Pispisa, Aggregation and water-membrane partition as major determinants of the activity of the antibiotic peptide trichogin GA IV, Biophys. J. 86 (2004) 936-945.

[26] R.F. Epand, R.M. Epand, V. Monaco, S. Stoia, F. Formaggio, M. Crisma, C. Toniolo, The antimicrobial peptide trichogin and its interaction with phospholipid membranes, Eur. J. Biochem. 266 (1999) 1021-1028.

[27] R.F. Epand, R. M. Epand, V. Monaco, S. Stoia, F. Formaggio, M. Crisma, C. Toniolo, The antimicrobial peptide trichogin and its interaction with phospholipid membranes, Eur. J. Biochem. 266 (1999) 1021-1028.

[28] A. D. Milov, R. I. Samoilova, Yu. D. Tsvetkov, V. A. Gusev, F. Formaggio, M. Crisma, C. Toniolo, J. Raap, Spatial distribution of spin-labeled trichogin GA IV in the Gram-positive bacterial cell membrane determined from PELDOR data, Appl. Magn. Reson. 23 (2002) 81-95.

[29] A. D. Milov, Yu. D. Tsvetkov, F. Formaggio, M. Crisma, C. Toniolo, G. L. Millhauser, J. Raap, Self-assembling properties of a membrane-modifying lipopeptaibol in weakly polar solvents studied by CW ESR, J. Phys. Chem. B 105 (2001) 11206-11212.

[30] M. E. Kardash, S. A. Dzuba, Communication: Orientational self-ordering of spin-labeled cholesterol analogs in lipid bilayers in diluted conditions, J Chem. Phys. 141 (2014) 211101/1-4.

[31] M.E. Kardash, S.A. Dzuba, Lipid-mediated clusters of guest molecules in model membranes and their dissolving in presence of lipid rafts, J. Phys. Chem. B 121 (2017) 5209-5217.

[32] V. Monaco, F. Formaggio, M. Crisma, C. Toniolo, P. Hanson, G. L. Millhauser, Orientation and immersion depth of a helical lipopeptaibol in membranes using TOAC as an ESR probe, Biopolymers 50 (1999) 239-253.

[33] M. De Zotti, B. Biondi, C. Peggion, F. Formaggio, Y. Park, K.-S. Hahm, C. Toniolo, Trichogin GA IV: a versatile template for the synthesis of novel peptaibiotics, Org. Biomol. Chem. 10 (2012) 1285-1299.

[34] S. Bobone, Y. Gerelli, M. De Zotti, G. Bocchinfuso, A. Farrotti, B. Orioni, F. Sebastiani, E. Latter, J. Penfold, R. Senesi, F. Formaggio, A. Palleschi, C. Toniolo, G. Fragneto, L. Stella, Membrane thickness and the mechanism of action of the short peptaibol trichogin GA IV, Biochim. Biophys. Acta - Biomembr. 1828 (2013) 1013-1024.

[35] A. D. Milov, Y. D. Tsvetkov, M. De Zotti, C. Prinzivalli, B. Biondi, F. Formaggio, C. Toniolo, M. Gobbo, Aggregation modes of the spin mono-labeled tylopeptin B and heptaibin peptaibiotics in frozen solutions of weak polarity as studied by PELDOR spectroscopy, J. Struct. Chem., 54(S1) (2013), S73-S85.

[36] A. Akbarzadeh, R. Rezaei-Sadabady, S. Davaran, S. W. Joo, N. Zarghami, Y. Hanifehpour, M. Samiei, M. Kouhi, K. Nejati-Koshki, Liposome: classification, preparation, and applications, Nanoscale Res. Lett. 8 (2013) 102/1-9.

[37] S.A. Dzuba, D. Marsh, ESEEM of Spin Labels to Study Intermolecular Interactions, Molecular Assembly and Conformation, in: A Specialist Periodic Report, Electron Paramagnetic Resonance, Vol. 24, 102–121 Eds. C. Gilbert, V. Chechik, D.M. Murphy, RSC Publishing (2015).

[38] A.D. Milov, Yu.A. Grishin, S.A. Dzuba, Yu.D. Tsvetkov, Effect of pumping pulse duration on echo signal amplitude in four-pulse PELDOR, Appl. Magn. Reson. 41 (2011) 59-67.

[39] H. J. Steinhoff, N. Radzwill, W. Thevis, V. Lenz, D. Brandenburg, A. Antson, G. Dodson, A. Wollmeri, Determination of interspin distances between spin labels attached to insulin: comparison of electron paramagnetic resonance data with the X-ray structure, Biophys. J. 73 (1997) 3287-3298.

[40] A. D. Milov, A. G. Maryasov, Yu. D. Tsvetkov, Pulsed electron double resonance (PELDOR) and its applications in free-radicals research, Appl. Magn. Reson. 15 (1998) 107-143.

[41] K. M. Salikhov, I. T. Khairuzhdinov, R. B. Zaripov, Three-pulse ELDOR theory revisited, Appl. Magn. Reson. 45 (2014) 573-619.

[42] D. A. Erilov, R. Bartucci, R. Guzzi, A. A. Shubin, A. G. Maryasov, D. Marsh, S. A. Dzuba, L. Sportelli, Water concentration profiles in membranes measured by ESEEM of spin-labeled lipids, J. Phys. Chem. B, 109 (2005) 12003-12013.

[43] A. D. Milov, R. I. Samoilova, A. A. Shubin, Yu. A. Grishin, S. A. Dzuba, ESEEM measurements of local water concentration in D_2O-containing spin-labeled systems, Appl. Magn. Reson. 35 (2008) 73-94.

[44] T. Kaneda, Iso-and anteiso-fatty acids in bacteria: biosynthesis, function, and taxonomic significance, Microbiol. Rev. 55 (1991) 288-302.

[45] (a) M. D. Resh, Palmitoylation of ligands, receptors, and intracellular signaling molecules, Sci. Stke, 359 (2006) re14. (b) M.E. Linder, in: Protein Lipidation, 215-240 (F. Tamanoi and D. Sigman, Eds, Academic Press, 2000, San Diego, CA).

[46] M. D. Resh, Regulation of cellular signalling by fatty acid acylation and prenylation of signal transduction proteins, Cell. Signal. 8 (1996) 403-412.

[47] R. P. Bazinet, S. Layé, Polyunsaturated fatty acids and their metabolites in brain function and disease, Nature Rev. Neurosci. 15 (2014) 771-785.

Peptide antibiotic trichogin in model membranes: self-association and capture of fatty acids

Ekaterina F. Afanasyeva,[a,b] Victoria N. Syryamina,[a,b] Marta De Zotti,[c] Fernando Formaggio,[c,d] Claudio Toniolo,[c,d] and Sergei A. Dzuba[a,b,*]

[a]Institute of Chemical Kinetics and Combustion, RAS, Novosibirsk 630090, Russian Federation

[b]Novosibirsk State University, Novosibirsk 630090, Russian Federation

[c]Department of Chemical Sciences, University of Padova, 35131 Padova, Italy

[d]Institute of Biomolecular Chemistry, Padova Unit, CNR, 35131 Padova, Italy

Abstract

The antimicrobial action of peptides in bacterial membranes is commonly related to their mode of self-assembling which results in pore formation. To optimize peptide antibiotic use for therapeutic purposes, a study on the concentration dependence of self-assembling process is thus desirable. In this work, we investigate this dependence for peptaibol trichogin GA IV (Tric) in the 1-palmitoyl-2-oleoyl-*sn*-glycero-3-phosphocholine (POPC) model membrane in the range of peptide concentrations between 0.5 and 3.3 mol %. Pulsed double electron-electron resonance (PELDOR) applied on spin-labeled peptide analogs highlights the onset of peptide dimerization above a critical peptide concentration value, namely ~ 2 mol %. Electron spin echo (ESE) envelope modulation (ESEEM) for D_2O-hydrated bilayers shows that dimerization is accompanied by peptide re-orientation towards a *trans*-membrane disposition. For spin-labeled stearic acids (5-DSA) in POPC bilayers, the study of ESE decays and ESEEM in the presence of a deuterated peptide analog indicates that above the critical peptide concentration the 5-DSA molecules are attracted by peptide molecules, forming nanoclusters. As the 5-DSA molecules represent a model for the behavior of fatty acids participating in bacterial membrane homeostasis, such capturing action by Tric may represent an additional mechanism of its antibiotic activity.

Keywords: dipolar spectroscopy, ESEEM, EPR, fatty acids, ion channels, PELDOR, trichogin

Introduction

The ever-increasing growth of antibiotic resistance in bacterial and fungal pathogens is a great challenge for modern medicine. Besides developing synthetic antibiotics of new generation, naturally-occurring antimicrobial agents and among them, antimicrobial peptides (AMPs) are generally considered as promising therapeutic agents [1]. Membrane-active peptides are a subclass of AMPs. They interact nonspecifically with bacterial membranes modifying their properties significantly, or even completely, retarding the onset of bacterial resistance. To optimize AMP design, a deep understanding of their mechanism of membrane destabilization would be extremely helpful.

The generally accepted mechanism for AMP membrane perturbation involves formation of channels or pores that increase ion and water flows through the lipid bilayer [2]. This phenomenon starts from peptide binding to lipid bilayer due to hydrophobic and electrostatic interactions. Then, peptides accumulate in the membrane and, after the peptide/lipid ratio attains a specific critical value, peptides self-associate in oligomers that eventually form channels. A precise knowledge of such critical peptide concentration value is highly desirable.

Besides, membrane perturbation processes may start at lower peptide concentration values. For example, at low concentrations peptides may still disrupt the local lipid chain packing and mobility [3]. A progressive membrane disordering was observed for different AMPs with increasing peptide concentration [4], and peptides were found able to enhance flip-flop lipid transitions between membrane leaflets and destroy cholesterol rafts in the membrane [5,6]. These perturbations influence the membrane thickness and flexibility [3,7-9].

Recently, we found peptide-induced redistribution of free fatty acids in the membrane mediated by the AMP alamethicin [10]. Free fatty acids are important components of

bacterial membranes because of their involvement in lipid homeostasis, protein functioning, signal transporting, and regulation functioning [11-13]. Therefore, redistribution of free fatty acids appears to be an alternative mechanism of peptide membrane-modifying action [10, 14].

Trichogin GA IV (Tric) is a natural undecapeptide (Scheme 1) isolated from the fungus *Trichoderma longibrachiatum*. Tric shows biological activity against Gram positive bacteria, has low hemolytic effect, and is stable to proteolysis [9,15,16]. 3D-Structural analysis indicated that Tric adopts a helical secondary structure [17-19], with a total peptide length of ~ 1.8-2.2 nm, that is about twice shorter than the lipid membrane thickness. A synthetic, covalent head-to-head Tric dimer exhibited a remarkably larger activity in comparison with the monomeric peptide [9]. Therefore, peptide self-assembling is required for pore formation by Tric.

Oligomerization of Tric results in transmembrane dimers [20,21]. Higher oligomers occur as well [22-25]. Tric self-association in the membrane is often accompanied by a change in peptide orientation from planar to transmembrane. However, for certain lipid compositions transmembrane oligomers are not formed even at high peptide concentrations [22, 26-28]. This phenomenon may be explained within the hypothesis of the carpet-like mechanism. Therefore, Tric membrane-perturbation mechanism is still under discussion.

Among other experimental techniques, pulsed EPR on spin-labeled molecules has proved to be a useful method to study peptide oligomerization and location in the membrane. Oligomerization may be investigated by pulsed electron-electron resonance [29], whereas location by electron spin echo (ESE) on deuterated systems using ESE envelope modulation method (^{2}H ESEEM) [20]. ESE decays can detect clusters of spin labels [10,30,31]. Conventional continuous wave (CW) EPR may provide complementary information as well.

Here, we employ CW and pulsed EPR techniques to study Tric, its partly deuterated analog ^{D}Tric, and the TOAC (1-oxyl-4-amino-2,2,6,6-tetramethylpiperidine-4-carboxylic acid) spin-labeled Tric analogs Tric^{1} and Tric^{8} (Scheme 1):

Scheme 1

*n*Oct-Aib-Gly-Leu-Aib-Gly-Gly-Leu-Aib-Gly-Ile-Leu-Lol (Tric)

*n*Oct(d_{15})-Aib-Gly-Leu(d_{10})-Aib-Gly-Gly-Leu(d_{10})-Aib-Gly-Ile(d_{10})-Lol (^{D}Tric)

*n*Oct-TOAC-Gly-Leu-Aib-Gly-Gly-Leu-Aib-Gly-Ile-Leu-Lol (Tric^{1})

nOct-Aib-Gly-Leu-Aib-Gly-Gly-Leu-TOAC-Gly-Ile-Leu-Lol (Tric^{8})

where *n*Oct is *n*-octanoyl, Aib is the non-proteinogenic α-aminoisobutyric acid, Lol is the 1,2-aminoalcohol leucinol and TOAC replaces Aib at either position 1 (Tric^{1}) or at position 8 (Tric^{8}). It is known that Aib→TOAC substitution does not alter the peptide membrane-modifying properties [27]. In the present study, all peptides are embedded in 1-palmitoyl-2-oleoyl-*sn*-glycero-3-phosphocholine (POPC) multilamellar vesicles.

Note that pulsed EPR studies on peptide location in model membranes was previously performed [20, 22] exploiting synthetic Tric analogs bearing the fluorescent, fluorenylmethyloxycarbonyl (Fmoc) group instead of the *n*Oct N$^{\alpha}$-blocking group [32].

In this work, we focus on two effects: (i) Tric self-assembling and (ii) Tric influence on the free fatty acid spatial distribution in POPC model membrane, using spin-labeled 5-doxyl-stearic acid (5-DSA) as a model for fatty acids.

Experimental

Sample preparation

The unlabeled peptide Tric and its partly deuterated analog ^{D}Tric were synthesized as described in [33, 34]. TOAC spin-labeled Tric analogs Tric^{1} and Tric^{8} were prepared by manual solid-phase peptide synthesis on a 2-chlorotrityl resin preloaded with Lol. The synthetic procedure followed for those two, new, TOAC-containing analogs closely resembles the one described in [35]. Tric^{1} and Tric^{8} were obtained in good yields (80% and 78%, respectively). The crude peptides were purified by medium-pressure liquid chromatography, by means of the Isolera Prime system Biotage (Sweden). POPC lipid was obtained from Avanti Polar Lipids (Birmingham, AL), 5-DSA was purchased from Sigma Aldrich (Germany). Methanol, ethanol and chloroform were Ekros-Analytica (St. Petersburg, Russia) products. A 10 mM phosphate buffered saline (PBS) containing 0.137 M NaCl and 0.0027 M KCl was used (pH = 7.0). In some cases, PBS was prepared with deuterated water. All commercial reagents were used without further purification.

Lipids, Tric analogs, and 5-DSA, taken at appropriate concentrations, were dissolved in chloroform. The solvent was slowly removed by nitrogen flow, followed by storage for 4 h *in vacuo* (10^{-2} bar). The dry lipid film was dispersed in buffer by vortex mixing. The amounts of buffer and lipid film were approximately the same (by weight). The sample was subjected to several cycles of rapid freezing-thawing. The large multilamellar vesicles (LMV) thus obtained [36] were kept at room temperature for 2 h and then transferred in a 5 mm o.d. tube (the sample length was about 5 mm), with 10% by weight dimethylsulfoxide added as a cryoprotector, and rapidly frozen in liquid nitrogen. The sample height did not exceed 5 mm.

EPR measurements

CW EPR experiments were carried out on an X-band Bruker ESP 380E EPR spectrometer using a dielectric Bruker ER 4118 X-MD-5 cavity and an Oxford Instruments CF-935 cryostat. The cryostat was cooled by nitrogen flow to 80 K. EPR spectra were

recorded at the modulation amplitude of 0.05 mT and modulation frequency of 100 kHz. The microwave power was set low enough to avoid spectra saturation.

All pulsed EPR experiments were carried out on an X-band Bruker ELEXSYS E580 EPR spectrometer equipped with a Bruker ER 4118 X-MD-5 cavity and an Oxford Instruments CF-935 cryostat. The cryostat was cooled by nitrogen flow to 80 K. Two-pulse echo decays, with the pulse sequence: $\pi/2$-τ-π-τ-*echo*, were obtained by scanning τ from 120 ns to 1.3 µs, with time steps of 4 ns. The ESE decay was measured at two different positions in the EPR spectra – at the maximum and the high-field shoulder of the echo-detected (ED) EPR spectra (see below). Three-pulse ESEEM experiments, with the pulse sequence: $\pi/2$-τ-$\pi/2$-T-$\pi/2$-τ-*echo*, were performed at the maximum of the ED-EPR spectra. The pulse lengths were 16 ns, τ was 204 ns, and the T interval was scanned from 248 ns to 10 µs with time steps of 12 ns. The data treatment was performed as described elsewhere [37]. A sixth-order polynomial fitting was applied to the relaxation decay in a semi-logarithmic plot. The modulus-Fourier transformation was performed on the normalized ESEEM decay using a MatLab home-made program.

Three-pulse PELDOR experiments were performed with the pulse sequence: $\pi/2_{(\nu A)}$-T-$\pi_{(\nu B)}$-(τ-T)-$\pi_{(\nu A)}$-τ-*echo*$_{(\nu A)}$, where the subscripts indicate two frequencies: one for detection (ν_A) and another for pumping (ν_B). The frequency offset ν_A-ν_B was 70 MHz, and ν_A and ν_B frequencies were chosen symmetrically around the center of the absorption dip in the resonator. The lengths of $\pi/2_{(\nu A)}$ and $\pi_{(\nu A)}$ pulses were 16 ns and 32 ns, respectively. The pumping pulse length was 32 ns. The amplitude of the $\pi_{(\nu B)}$ pulse was set to inverse the *echo*$_{(\nu A)}$ signal at the maximum of the echo-detected EPR spectra. The time τ was 800 ns. The time delay T for the pumping pulse was initially set to the negative value of -188 ns and then scanned with time intervals of 4 ns. The phase jumps due to the passage of the pumping $\pi_{(\nu B)}$

pulse through to the $\pi/2_{(vA)}$ pulse were eliminated by measuring the PELDOR decay for the samples without dipolar coupling [38].

Results

CW EPR of Tric[1] and Tric[8]: peptide self-association

Fig. 1 shows the CW EPR spectra recorded for the spin-labeled Tric[1] and Tric[8] at different peptide concentrations in POPC bilayers, at 80 K. One can see that an increase in peptide concentration results in line broadening, that clearly manifests itself in a relative decrease of the narrowest central component as compared with the wider low- and high-field components. For immobilized spin labels at low temperature, this broadening is induced by an electron-electron spin-spin dipole-dipole (d-d) interaction between spin labels [39]. The decrease of the central component seen for Tric[1] at a concentration of 3.3 mol % is larger than that seen for Tric[8] at a concentration of 5 mol %. This finding provides evidence that both peptides self-associate through contacts involving their N-terminal region.

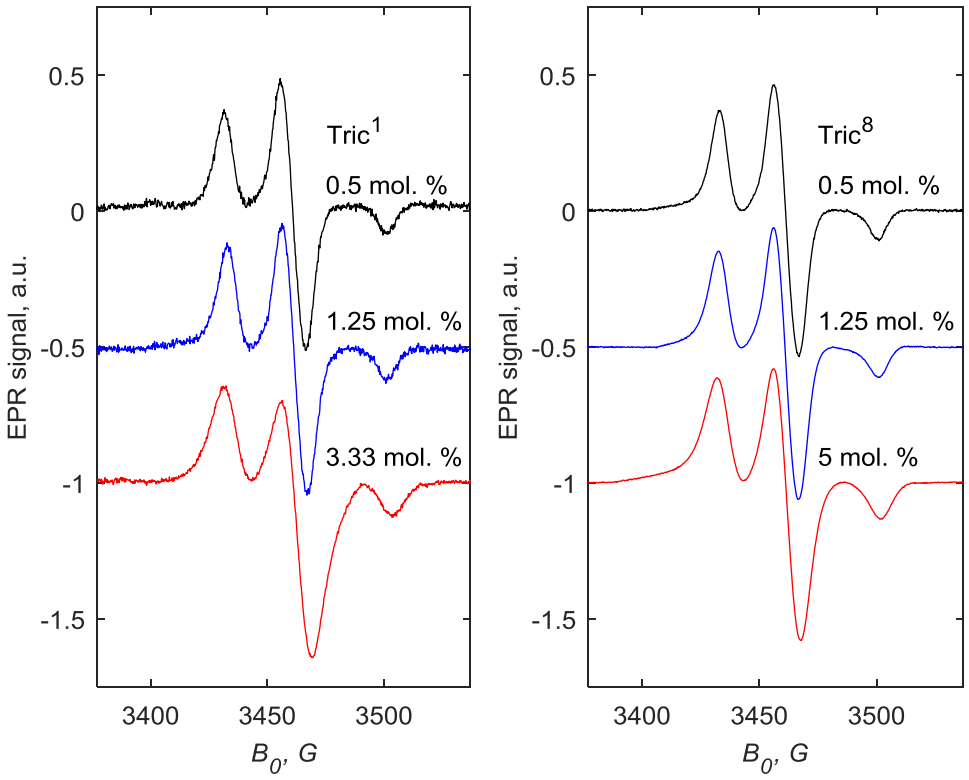

Fig. 1. CW EPR spectra of Tric[1] and Tric[8] in POPC bilayers taken at different peptide concentrations. Spectra are shifted along the vertical scale for convenience. Temperature: 80 K.

PELDOR of Tric[1] and Tric[8]: peptide dimerization

We obtained detailed information on spin label clustering using the PELDOR technique. PELDOR experiments with spin-labeled Tric analogs Tric[1] and Tric[8], were carried out at several peptide concentrations. The representative PELDOR signal dependences on the time delay *T* are shown in Fig. 2. Note that the large CW EPR line broadening observed for Tric[1] at 3.3 mol % concentration (Fig. 1) implies that in this case PELDOR data cannot be considered reliable, because of fast signal decay due to d-d interactions.

The PELDOR signal, $V(T)$, is caused by d-d interactions between spin labels. For nanoscale clusters, these interactions are of two independent types, namely between

molecules associated in a cluster and between different clusters. Then, $V(T)$ may be presented as a product of two independent factors, $V_{INTRA}(T)$ and $V_{INTER}(T)$:

$$V(T) = V_{INTRA}(T) * V_{INTER}(T) \quad (1)$$

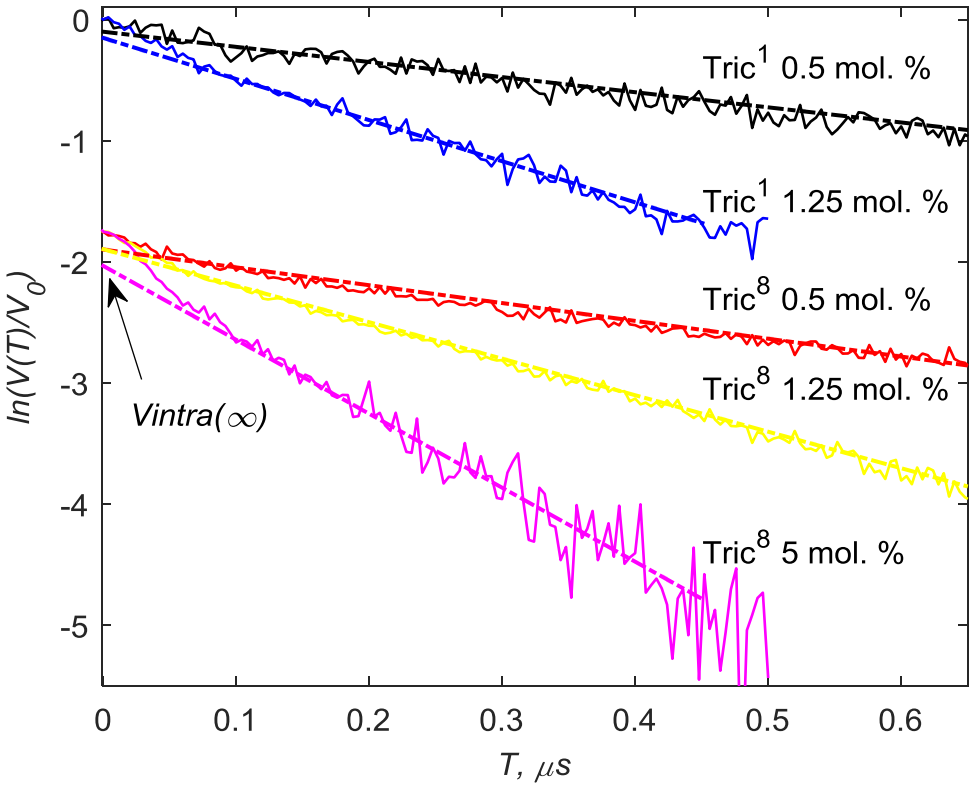

Fig. 2. Semi-logarithmic plot of representative PELDOR signal time dependences $V(T)$ at different peptide concentrations for Tric[1] and Tric[8]. Data for Tric[8] are shifted downwards for convenience. The dashed straight lines show linear asymptotes. Temperature: 80 K.

For a nanocluster formed by spin-labeled molecules, $V_{INTRA}(T)$ attains an asymptotic value [40]:

$$V_{INTRA}(\infty) = (1 - p_B)^{n-1}, \quad (2)$$

where p_B is the efficiency of the microwave excitation at the pumping frequency ν_B and n is the number of molecules in the cluster.

For a random spin-label distribution in the 3D-space, the $V_{INTER}(T)$ temporal dependence is a simple exponential:

$$V_{INTER}(T) = V_0 \exp\left(-\frac{4\pi^2}{9\sqrt{3}}\frac{g^2\mu_B{}^2}{\hbar}Cp_BT\right) \quad (3)$$

where g is the g-factor, μ_B is the Bohr magneton, C is the volume spin-label concentration (in cm^{-3}). Eq. (3) predicts that in the coordinates of Fig. 2 the $V(T)$ time dependence, after $V_{INTRA}(T)$ arrived to its asymptotic value, is expected to obey a linear dependence. This phenomenon is indeed observed (dashed lines in this plot).

From extrapolation of the dashed lines in Fig. 2 the $V_{INTRA}(\infty)$ value can be obtained. In turn, it provides the mean number n in a cluster by use of Eq. (2), if p_B is known. This latter value is calculated by taking into account the overlapping of excitation bandwidths for the A and B spins [41]:

$$p_B = \frac{p_B^0}{1 - p_A^0}$$

where

$$p_{B(A)}^0 = \int_0^\infty \frac{\omega_1^2}{\omega_1^2 + (\omega - \omega_{B(A)})^2} \sin^2\left(\frac{t_p}{2}\sqrt{\omega_1^2 + (\omega - \omega_{B(A)})^2}\right) A(\omega) d\omega \approx 2\omega_1 A(\omega_{B(A)}), \quad (4)$$

where $A(\omega)$ is a function describing the spin-label EPR absorptive lineshape (with the integral normalized to unity), $\omega_{B(A)} = 2\pi\nu_{B(A)}$, ω_1 is the microwave amplitude, and t_p is the pumping pulse length; the given approximate estimation for $p_{B(A)}^0$ is valid for $\omega_1 t_p = \pi$ and ω_1 smaller than spectral linewidth. Previously [14], it was shown that this approach provides good agreement with experiment.

Employing the obtained data on $V_{INTRA}(\infty)$ values and Eq. (2), the *n* values were found. As these values were not integer numbers, a mixture of monomers and dimers should be assumed to be present in the samples. So, instead of *n*, it would be more reasonable to use a mean number <*n*>. The results of <*n*> calculations are shown in Fig. 3. One can see that at small peptide concentrations the dependence is linear (and similar for both Tric[1] and Tric[8] analogs), while a saturated-like behavior is observed at higher concentrations. A tenfold increase in peptide concentration (from 0.5 to 5 mol %) results in the <*n*> value rising from 1.15 ± 0.03 (at 0.5 mol %) to 1.90 ± 0.07 (at 5 mol %). Such findings prove that at low concentrations mostly peptide monomers are present while at high concentrations dimers are prevailing.

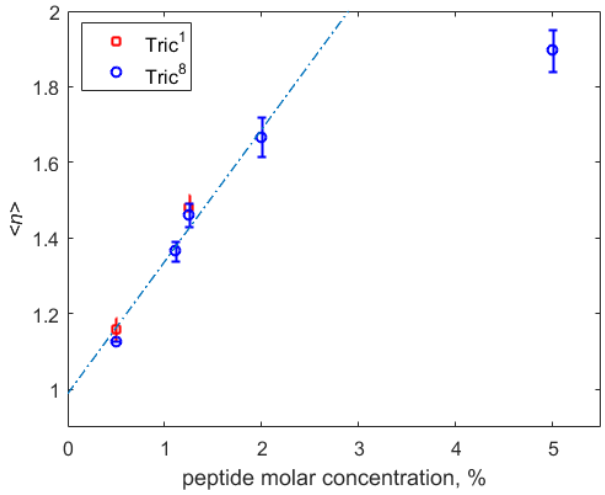

Fig. 3. Mean number <*n*> of self-associated peptide molecules obtained using Eq. (2) from the PELDOR data (shown in Fig. 2). The straight dash-dotted line indicates a linear dependence at low concentrations.

^{2}H ESEEM for Tric^1 and Tric^8 upon D_2O-hydration: peptide location in the bilayer

Information on the location of spin-labeled peptides in the membrane can be obtained from ESEEM experiments on D_2O-hydrated bilayers [14, 20, 37]. The ^{2}H ESEEM signal in this approach depends on the distance between the spin label and the deuterium nuclei [42].

So the closer the spin label is to the membrane surface, the larger the ^{2}H ESEEM line intensity is expected. The measurements performed in this work for Tric^{1} and Tric^{8} resulted in frequency-domain ESEEM spectra looking similar to those presented in [14]. The spectra show a narrow line positioned at 2.2 MHz, that is the deuterium Larmor frequency (at the microwave X-band). The experimentally obtained intensities for the narrow line A_N (see definition in [14], Fig. 6 therein) at low, ~ 0.5 mol %, and large, ~ 5 mol %, peptide concentrations are given in Table 1. Literature data [20-22] for closely-related, spin-labeled Tric analogs in membrane bilayers of different lipid compositions are also reported in Table 1 for comparison. Note that the spin-labeled Tric analogs studied in the cited papers [and herein termed: Fmoc-Tric^{1}-OMe and Fmoc-Tric^{8}-OMe (OMe, methoxy)] carried an N-terminal Fmoc- instead of the native *n*Oct- group, and a leucine methyl ester at their C-terminus (instead of the naturally-occurring 1,2-aminoalcohol Lol).

Table 1. Intensity of the ^{2}H ESEEM line at the deuterium Larmor frequency, A_N/MHz^{-1}, for Tric^1 and Tric^8 peptide analogs in D_2O-hydrated bilayers at two peptide concentrations

Peptide / Bilayer	Tric^1, 0.5 mol %	Tric^1, 5 mol %	Tric^8, 0.5 mol %	Tric^8, 5 mol %	Reference
POPC	**0.036**	**0.031**	**0.020**	**0.027**	**This work**
POPC	0.086	0.0515	0.052	0.047	[21]*
ePC**/cholesterol	0.12	0.05	0.12	0.12	[22]*
DPPC**	0.10	0.05	0.07	0.05	[20]*,***

The experimental uncertainty is not larger than 10 %.

*These data refer to the two Tric analogs Fmoc-Tric^1-OMe and Fmoc-Tric^8-OMe.

**ePC is egg phosphatidylcholine and DPPC is 1,2-dipalmitoyl-sn-glycero-3-phosphocholine.

***A_N in arbitrary units.

Data in Table 1 show that substitution of *n*Oct by Fmoc results in larger A_N values. This finding implies that Fmoc-Tric^1-OMe and Fmoc-Tric^8-OMe are located closer to the bilayer surface than Tric^1 and Tric^8. For Tric^1, A_N decreases by a factor of 1.16 with increasing concentration, while for Tric^8 it increases by a factor of 1.35. This means that, while the peptide concentration increases, the label at position 1 becomes more inserted into the membrane while that at position 8 becomes closer to the membrane surface. Both findings point towards a peptide reorientation upon increasing concentration.

This behavior is to be compared with that of Fmoc-Tric^1-OMe and Fmoc-Tric^8-OMe in different lipid bilayers, where (as the peptide concentration increases) a greater decrease in A_N value is registered for the spin-label at position 1 under all experimental conditions

(decrease factors from 1.7 to 2.2), while for the spin label at position 8 unchanged or slightly lower A_N values (decrease factor of ~ 1.3) are registered.

In conclusion, an increase in peptide concentration results in (i) a deeper insertion in the lipid bilayer of the N-terminal part of the peptide for Fmoc-containing analogs than *n*Oct-containing ones (that are less deeply inserted). (ii) The peptide C-terminus is somewhat exposed on the bilayer surface for *n*Oct-containing analogs, while slightly buried into it for Fmoc-containing ones.

ESE decays for 5-DSA in presence of 'native' Tric: clustering of fatty acids

CW EPR spectra recorded for 5-DSA in POPC bilayers showed the typical lineshape for immobilized nitroxide spin labels. Upon (*unlabelled*) Tric addition, the EPR spectra did not change noticeably, showing only a slight line broadening in response to increasing peptide concentration, as a result of dipole-dipole (d-d) interactions (similar to those published in [31]). Thus, we decided to apply ESE to study d-d interactions between 5-DSA molecules, since ESE decays are known to be much more sensitive to d-d interactions than CW EPR spectra.

In the nanoscale range of distances, d-d interactions between spin labels can be readily detected by measuring the "instantaneous spectral diffusion" effect [31] in ESE decays. This effect takes place because the microwave pulses "instantly" flip the magnetic dipolar field (acting on the selected spin by a coupled spin). This effect results in an additional defocusing of the ESE signal. (Note that PELDOR spectroscopy is based on the same physical principle, but the flip of the magnetic dipolar field is performed applying pulses at different microwave frequencies). ESE decays are sensitive to nanoscale local concentrations because d-d interactions matter up to distances r (determined by the relation $r \sim \sqrt[3]{\gamma^2 \hbar \tau}$) of about 10 nm, as in organic solids τ is typically in the μs time range.

In the case of a random 3D-space distribution, this mechanism results in the same analytical formula as Eq. (3), with time T replaced by 2τ, $\omega_A = \omega_B$ (the excitation and detection frequencies are the same), and $p_A^0 = 0$. Spin labels in 5-DSA molecules embedded into membranes are expected to exhibit a 2D-space distribution (in the case of Tric[1] and Tric[8], the spin label locations may remarkably deviate from the in-plane position, so that in this case a 3D-distribution is preferable). Instead of Eq. (3), the ESE decays for a 2D-distribution are described fairly well by the approximated formula [31]:

$$E_{2D}(\tau) \cong E_0 \exp\{-3.21\sigma p_B (g^2\mu_B^2\tau/\hbar)^{\frac{2}{3}}\} \quad (5)$$

where σ is the spin label surface concentration measured in cm^{-2} units. Therefore, we can obtain the local surface concentration σ of spin-labeled molecules directly from the ESE decays, by plotting $\ln(E_{2D}(\tau))$ as a function of $\tau^{\frac{2}{3}}$.

However, the ESE signal decays through many different relaxation mechanisms. To refine the pure contribution of the instantaneous diffusion effect, one should perform measurements with different p_B values, because at cryogenic temperatures the other relaxation mechanisms are expected to be independent of this parameter. From Eq. (4), it follows that this study can be carried out by measuring ESE decays at two different spectral positions. For ESE decays obtained at two field positions and divided by each other, the p_B parameter in Eq. (5) should be replaced by the difference $[p_B(1) - p_B(2)]$, where numbers in parenthesis denote the two field positions.

Fig. 4 shows the ratio between echo time traces obtained at the two field positions (indicated by arrows in the figure inset). Data are given for 5-DSA at 1 mol. % concentration in the POPC bilayer, as a function of increasing Tric concentration (from 0 to 3.3 mol %). The coordinates employed are convenient for comparison with Eq. (5). The small oscillations

seen in the curves are ESEEM induced by electron-nuclear interactions with the neighboring proton spins. Fig. 4 shows that the echo decays obey the $\tau^{\frac{2}{3}}$ time dependence predicted by Eq. (5).

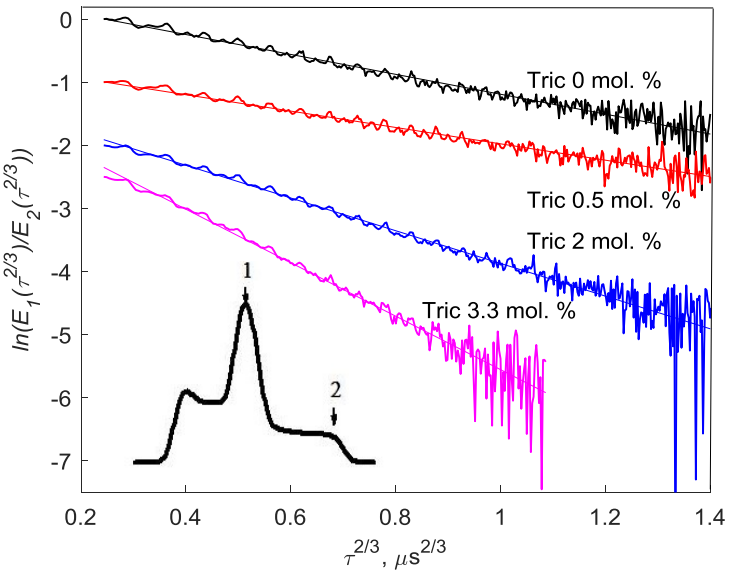

Fig. 4. Ratio between ESE time traces taken for 5-DSA in POPC bilayers at two field positions in the EPR spectrum (as indicated by arrows in the inset) at different Tric concentrations. Data are plotted in the coordinates suitable for comparison with Eq. (5). Curves are shifted along the vertical axis for convenience. The 5-DSA concentration is 1 mol %. Measurements were performed at 80 K.

ESE decays in Fig. 4 depend remarkably on Tric concentration. To employ the theoretical Eq. (5), the parameter $[p_B\ (1) - p_B\ (2)]$ must be determined. This calculation was carried out as described in [14]. The value found for this parameter is 0.19 ± 0.02. Then, applying Eq. (5) to the linear dependences in Fig. 4, we obtained the surface densities σ. These data are plotted in Fig. 5 as a function of Tric concentration, in dimensionless units by dividing σ by the host lipid lateral density in the bilayer, σ_0. The latter parameter was

estimated to be $\sigma_0 \approx 1.7\,10^{14}$ cm^{-2} (see [31] for details), that corresponds to the mean area per lipid ~ 0.60 nm^2.

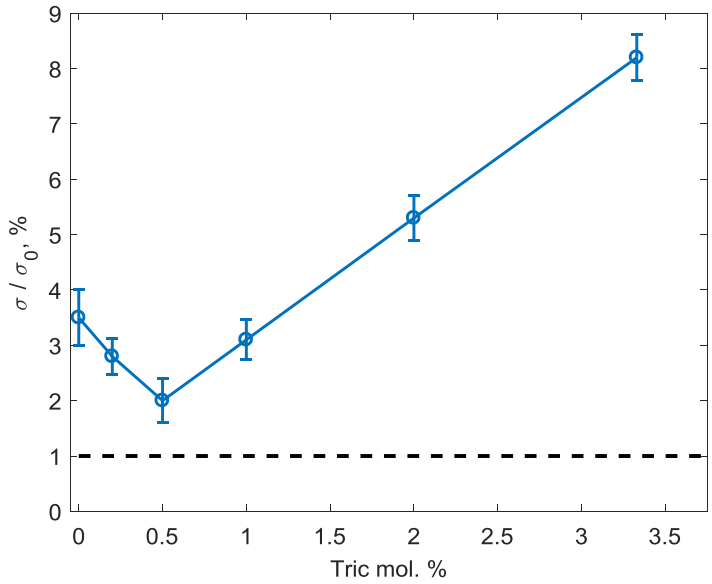

Fig. 5. 5-DSA surface concentration σ in the presence of Tric in POPC bilayers, as a function of increasing peptide concentration, as obtained from the slopes reported in Fig. 4. The solid lines are drawn to guide the eye. The mean 5-DSA concentration (1 mol %) in the bilayer is indicated by the horizontal dashed line.

Data in Fig. 5 clearly indicate that the σ value largely exceeds the mean free fatty acid concentration (1 mol %) in the bilayer. This enhancement unambiguously highlights that 5-DSA molecules form lateral clusters in the bilayer. These clusters are formed even in the absence of Tric. This finding is in agreement with our previous data [10, 31]. Fig. 5 shows that, as the Tric concentration increases, clusters are first destroyed (this effect is however small) and then, with a further peptide concentration increase (above 1 mol %), the clusters becomes larger and/or denser. One may conclude therefore that peptide promotes cluster formation.

ESEEM for 5-DSA in presence of ^{D}Tric: peptide captures fatty acids

We suggest that the experimentally found noticeable increase of the local 5-DSA concentration in the bilayer in the presence of Tric is essentially the result of a mutual attraction between fatty acids and Tric molecules, with formation of a 5-DSA nanocluster around the peptide. To support this hypothesis, ESEEM experiments were performed for 5-DSA with the deuterated peptide ^{D}Tric (Scheme 1). The ^{2}H-ESEEM effect is known to be detected when the unpaired electron of a spin label and the deuterium nucleus are separated by a distance no longer than 0.8 - 1 nm [43]. Clearly, this experiment can provide a good evidence for a close contact between 5-DSA and Tric molecules.

The ^{2}H ESEEM data obtained for 5-DSA in POPC bilayer at different ^{D}Tric peptide concentrations are reported in Fig. 6. The ESEEM spectra in the frequency domain show a narrow line positioned at 2.2 MHz (Fig. 6, left) assigned to the deuterium Larmor frequency (at the X-band). Data in Fig. 6 (right) show that A_N increases with increasing peptide concentration until 2 mol % peptide concentration. Then, a plateau is reached at larger peptide concentrations.

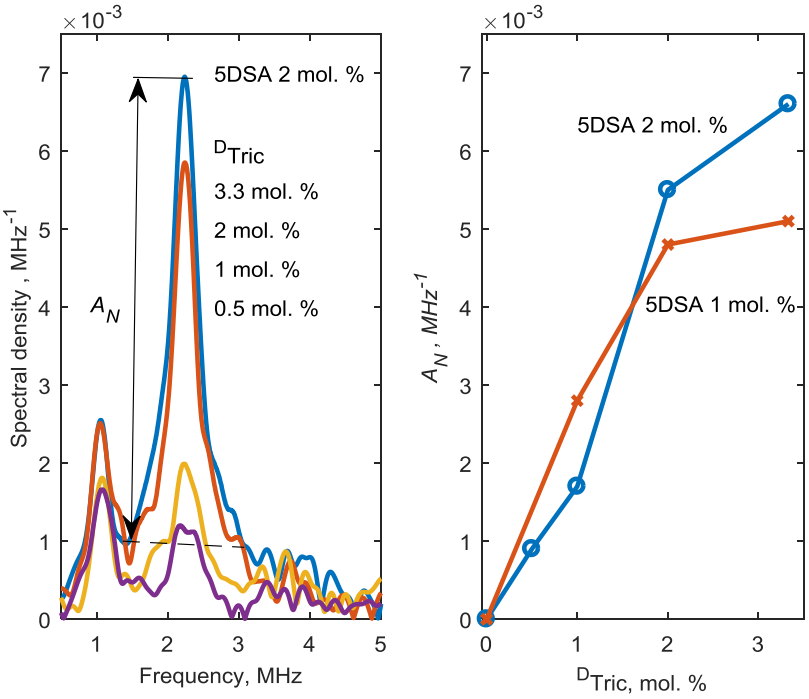

Fig. 6. Left: ^{2}H ESEEM spectra for 5-DSA in POPC bilayers at different ^{D}Tric concentrations. Right: the 2.2 MHz line intensity as a function of ^{D}Tric concentration, at 1 mol% and 2 mol % 5-DSA concentrations.

For the putative case of a random 5-DSA spatial distribution in the membrane, one can estimate that for 1 mol % 5-DSA concentration the mean distance between molecules is around ~ 7 nm. This value is significantly larger than that of 1 nm [43] which represents the upper boundary for the onset of the ^{2}H ESEEM effect. Therefore, the effect presented in Fig. 6 unambiguously proves that peptides capture fatty acids. Taking into account the data described above on the ESE decays for 5-DSA in the presence of *unlabelled* Tric, this capture results in a clustering of the 5-DSA molecules around the peptides.

Discussion

Peptide dimerization and location

PELDOR data in Figs. 2 and 3 clearly demonstrate that peptides form dimers. CW EPR data in Fig. 1 show that dimerization occurs through interaction of two N-termini (head-to-head dimerization). This result is in agreement with previous PELDOR data on the Fmoc-Tric^{1}-OMe and Fmoc-Tric^{8}-OMe peptide analogs [20,21] where the authors reported n = 2.1 ± 0.1 at 5 mol % peptide concentration [20]. These dimers possibly induce membrane leakage [21].

The dependence of the mean number <n> of peptide molecules in the self-associated species on peptide concentration seen in Fig. 3 may be interpreted with the onset of an equilibrium between peptide monomers and dimers in the membrane. The critical peptide concentration value where dimers become dominating is ~ 2 mol %.

ESEEM data on D_2O-hydrated bilayers (Table 1) demonstrate that Tric^{1} and Tric^{8} molecules are located deeper in the membrane core than Fmoc-Tric^{1}-OMe and Fmoc-Tric^{8}-OMe analogs (the A_N values in the former case are smaller). We explain this difference by noting that the bulkier and more rigid Fmoc- group in the latter analogs may reasonably cause a deeper peptide insertion into the membrane core. Data in Table 1 also show that as concentration increases, peptide molecules change their orientation in the membrane, with the N-terminus going deeper into the membrane interior and the C-terminus moving closer to the membrane surface. Note that a slight tendency for *n*Oct-Tric^{1}-OMe inserting in the membrane core and for *n*Oct-Tric^{8}-OMe moving to the membrane surface was also observed in [32].

Capturing of fatty acids

Fig. 4 shows that d-d-induced ESE decays for 5-DSA molecules obey the theoretical expression (5) which predicts a proportionality to $(\gamma^2 \hbar\, \tau)^{2/3}$. This behavior means that the spin labels in the 5-DSA molecules possess a 2D-distribution, as one may naturally expect for a

bilayer. Eq. (5) allows one to directly obtain the surface density σ. The calculated σ values deviate from those expected for homogeneously distributed molecules (Fig. 5). This effect, previously reported for POPC bilayers [10, 31], and DPPC and DOPC (1,2-dioleoyl-*sn*-glycero-3-phosphocholine) bilayers [31], is interpreted by formation of 5-DSA molecular nanoclusters. The 5-DSA local concentration in such clusters increases with increasing peptide concentration. The results in Fig. 5 indicate that peptides promote cluster formation.

This phenomenon is confirmed by ^{2}H ESEEM experiments on 5-DSA in the presence of ^{D}Tric (Fig. 6), where A_N is seen to strongly increase with increasing 5-DSA concentration (with saturation occurring above 2 mol %). Thus, one may conclude that 5-DSA clusters are formed around the peptide molecules. By comparison with the results of a previous computer modelling study [31] we can state that the size of such clusters is larger than 20 nm (below this value, the time traces in Fig. 4 are expected to become stretched – see Fig. 1 in [31]).

It is interesting to note that this nanocluster formation around peptide molecules occurs in the same concentration range where dimers are formed, namely around a peptide concentration of ~ 2 mol % (Fig. 3). Probably, peptide dimers disrupt the neighbor lipid packing and stearic acid molecules compensate for this perturbation.

Free fatty acids are building blocks for lipids and a component of bacterial membranes that regulates its physical properties such as a fluidity and rigidity [44]. Fatty acids also facilitate peptide/protein "anchoring" and traffic along the membrane by palmitoylation, a type of covalent attachment of free fatty acids to specific amino acids [45], that is relevant for peptide and protein functioning [11-13,45], and participate in signal transporting and regulation functioning [46, 47]. In summary, redistribution of free fatty acids seems to be an alternative mechanism by which peptides exert their membrane-modifying action [10,14].

Conclusion

In this work we studied two effects by which peptide antibiotic Tric perturbs the lipid membrane. The first effect involves peptide self-assembling to dimers which may induce membrane leakage. In the second, capture of free fatty acids by peptide molecules takes place in the bilayer, possibly leading to a disturbance of lipid homeostasis in the bacterial membrane. Both processes become effective above a critical peptide concentration, found to be around 2 mol % for Tric.

Below that critical concentration, the peptide molecules occur in the monomeric state in the membrane and free fatty acids form local clusters. At low peptide concentrations, both fatty acid clusters and peptides exist independently. Above the critical peptide concentration, Tric tends to form dimers, while clusters of fatty acids become denser, with a simultaneous mutual attraction between fatty acid clusters and peptides taking place. As free fatty acids are involved in membrane functioning, this capturing effect may perturb the physiological functions of the membrane and thus play an important role in peptide antibiotic action.

Acknowledgements

This work was supported by the Russian Science Foundation, project No. 15-15-00021. VNS is grateful to the Russian Foundation for Basic Research for its support with project # 17-44-543240. MDZ and FF gratefully acknowledge MIUR for financial support (FIRB 2013: project No. RBFR13RQXM and PRIN 2015: project No. 20157WW5EH).

References

[1] (a) K.A. Brogden, Antimicrobial peptides: pore formers or metabolic inhibitors in bacteria? Nature Rev. Microbiol. 3 (2005) 238-250; (b) K.V.R. Reddy, R.D. Yedery, C. Aranha, Antimicrobial peptides: premises and promises, Int. J. Antimicrob. Agents 24 (2004) 536-547.

[2] (a) M.S. Sansom, Alamethicin and related peptaibols: model ion channels, Eur. Biophys. J. 22 (1993) 105-124. (b) P. Tieleman, J. Bentz, Molecular dynamics simulation of the evolution of hydrophobic defects in one monolayer of a phosphatidylcholine bilayer: relevance for membrane fusion mechanisms, Biophys. J. 83 (2002) 1501-1510. (c) O.S. Andersen, R.E. Koeppe, B. Roux, Gramicidin channels, IEEE, Trans. Nanobiosci. 4 (2005) 10-20.

[3] A.J. Costa-Filho, Y. Shimoyama, J.H. Freed, A 2D-ELDOR study of the liquid ordered phase in multilamellar vesicle membranes, Biophys. J. 84 (2003) 2619-2633.

[4] M. Bortolus, A. Dalzini, C. Toniolo, K.-S. Hahm, A.L. Maniero, Interaction of hydrophobic and amphipathic antimicrobial peptides with lipid bicelles, J. Pept. Sci. 20 (2014) 517-525.

[5] S. Qian, W.T. Heller, Peptide-induced asymmetric distribution of charged lipids in a vesicle bilayer revealed by small-angle neutron scattering, J. Phys. Chem. B 115 (2011) 9831-9837.

[6] S. Qian, D. Rai, W.T. Heller, Alamethicin disrupts the cholesterol distribution in dimyristoyl phosphatidylcholine–cholesterol lipid bilayers, J. Phys. Chem. B 118 (2014) 11200-11208.

[7] L.I. Horvath, P.J. Brophy, D. Marsh, Exchange rates at the lipid-protein interface of myelin proteolipid protein studied by spin-label electron spin resonance, Biochemistry 27 (1988) 46-52.

[8] B. Bechinger, The structure, dynamics and orientation of antimicrobial peptides in membranes by multidimensional solid-state NMR spectroscopy, Biochim. Biophys. Acta - Biomembr. 1462 (1999) 157-183.

[9] C. Toniolo M. Crisma, F. Formaggio, C. Peggion, V. Monaco, C. Goulard, S. Rebuffat, B. Bodo, Effect of N^{α}-acyl chain length on the membrane-modifying properties of synthetic analogs of the lipopeptaibol trichogin GA IV, J. Am. Chem. Soc. 118 (1996) 4952-4958.

[10] E. F. Afanasyeva, V. N. Syryamina, S. A. Dzuba, Communication: Alamethicin can capture lipid-like molecules in the membrane, J. Chem. Phys. 146 (2017) 011103/1-4.

[11] D.D. Martin, E. Beauchamp, L.G. Berthiaume, Post-translational myristoylation: fat matters in cellular life and death, Biochimie 93 (2011) 18-31.

[12] Y.-M. Zhang, C.O. Rock, Membrane lipid homeostasis in bacteria, Nat. Rev. Microbiol. 6 (2008) 222-233.

[13] A.W. Smith, Lipid-protein interactions in biological membranes: a dynamic perspective Biochim. Biophys. Acta - Biomembr. 1818 (2012) 172-177.

[14] V.N. Syryamina, M. De Zotti, C. Toniolo, F. Formaggio, S.A. Dzuba, Alamethicin self-assembling in lipid membranes: concentration dependence from pulsed EPR of spin labels, Phys. Chem. Chem. Phys. 20 (2018) 3592-3601.

[15] M. De Zotti, B. Biondi, F. Formaggio, C. Toniolo, L. Stella, Y. Park, K.-S. Hahm, Trichogin GA IV: an antibacterial and protease-resistant peptide, J. Pept. Sci. 15 (2009) 615-619.

[16] M. De Zotti, B. Biondi, Y. Park, K.-S. Hahm, M. Crisma, C. Toniolo, F. Formaggio, Antimicrobial lipopeptaibol trichogin GA IV: role of the three Aib residues on conformation and bioactivity, Amino Acids 43 (2012) 1761-1777.

[17] C. Toniolo, C. Peggion, M. Crisma, F. Formaggio, X. Shui, D. S. Eggleston, Structure determination of racemic trichogin A IV using centrosymmetric crystals, Nat. Struct. Mol. Biol. 1 (1994) 908-914.

[18] D. J. Anderson, P. Hanson, J. Mc Nulty, G. L. Millhauser, V. Monaco, F. Formaggio, M. Crisma, C. Toniolo, Solution structures of TOAC-labeled trichogin GA IV peptides from allowed ($g \approx 2$) and half-field electron spin resonance, J. Am. Chem. Soc. 121 (1999) 6919-6927.

[19] A. D. Milov, A. G. Maryasov, Yu. D. Tsvetkov, J. Raap, Pulsed ELDOR in spin-labeled polypeptides, Chem. Phys. Lett. 303 (1999) 135-143.

[20] E. S. Salnikov, D. A. Erilov, A. D. Milov, Yu. D. Tsvetkov, C. Peggion, F. Formaggio, C. Toniolo, J. Raap, S. A. Dzuba, Location and aggregation of the spin-labeled peptide trichogin GA IV in a phospholipid membrane as revealed by pulsed EPR, Biophys. J. 91 (2006) 1532-1540.

[21] V. N. Syryamina, N. P. Isaev, C. Peggion, F. Formaggio, C. Toniolo, J. Raap, S. A. Dzuba, Small-amplitude backbone motions of the spin-labeled lipopeptide trichogin GA IV in a lipid membrane as revealed by electron spin echo, J. Phys. Chem. B 114 (2010) 12277-12283.

[22] V. N. Syryamina, M. De Zotti, C. Peggion, F. Formaggio, C. Toniolo, J. Raap, S. A. Dzuba, A molecular view on the role of cholesterol upon membrane insertion, aggregation, and water accessibility of the antibiotic lipopeptide trichogin GA IV as revealed by EPR, J. Phys. Chem. B 116 (2012) 5653-5660.

[23] M. Smetanin, S. Sek, F. Maran, J. Lipkowski, Molecular resolution visualization of a pore formed by trichogin, an antimicrobial peptide, in a phospholipid matrix, Biochim. Biophys. Acta – Biomembr. 1838 (2014) 3130-3136.

[24] T. N. Kropacheva, J. Raap, Voltage-dependent interaction of the peptaibol antibiotic zervamicin II with phospholipid vesicles, FEBS Lett. 460 (1999) 500-504.

[25] L. Stella, C. Mazzuca, M. Venanzi, A. Palleschi, M. Didonè, F. Formaggio, C. Toniolo, B. Pispisa, Aggregation and water-membrane partition as major determinants of the activity of the antibiotic peptide trichogin GA IV, Biophys. J. 86 (2004) 936-945.

[26] R.F. Epand, R.M. Epand, V. Monaco, S. Stoia, F. Formaggio, M. Crisma, C. Toniolo, The antimicrobial peptide trichogin and its interaction with phospholipid membranes, Eur. J. Biochem. 266 (1999) 1021-1028.

[27] R.F. Epand, R. M. Epand, V. Monaco, S. Stoia, F. Formaggio, M. Crisma, C. Toniolo, The antimicrobial peptide trichogin and its interaction with phospholipid membranes, Eur. J. Biochem. 266 (1999) 1021-1028.

[28] A. D. Milov, R. I. Samoilova, Yu. D. Tsvetkov, V. A. Gusev, F. Formaggio, M. Crisma, C. Toniolo, J. Raap, Spatial distribution of spin-labeled trichogin GA IV in the Gram-positive bacterial cell membrane determined from PELDOR data, Appl. Magn. Reson. 23 (2002) 81-95.

[29] A. D. Milov, Yu. D. Tsvetkov, F. Formaggio, M. Crisma, C. Toniolo, G. L. Millhauser, J. Raap, Self-assembling properties of a membrane-modifying lipopeptaibol in weakly polar solvents studied by CW ESR, J. Phys. Chem. B 105 (2001) 11206-11212.

[30] M. E. Kardash, S. A. Dzuba, Communication: Orientational self-ordering of spin-labeled cholesterol analogs in lipid bilayers in diluted conditions, J Chem. Phys. 141 (2014) 211101/1-4.

[31] M.E. Kardash, S.A. Dzuba, Lipid-mediated clusters of guest molecules in model membranes and their dissolving in presence of lipid rafts, J. Phys. Chem. B 121 (2017) 5209-5217.

[32] V. Monaco, F. Formaggio, M. Crisma, C. Toniolo, P. Hanson, G. L. Millhauser, Orientation and immersion depth of a helical lipopeptaibol in membranes using TOAC as an ESR probe, Biopolymers 50 (1999) 239-253.

[33] M. De Zotti, B. Biondi, C. Peggion, F. Formaggio, Y. Park, K.-S. Hahm, C. Toniolo, Trichogin GA IV: a versatile template for the synthesis of novel peptaibiotics, Org. Biomol. Chem. 10 (2012) 1285-1299.

[34] S. Bobone, Y. Gerelli, M. De Zotti, G. Bocchinfuso, A. Farrotti, B. Orioni, F. Sebastiani, E. Latter, J. Penfold, R. Senesi, F. Formaggio, A. Palleschi, C. Toniolo, G. Fragneto, L. Stella, Membrane thickness and the mechanism of action of the short peptaibol trichogin GA IV, Biochim. Biophys. Acta - Biomembr. 1828 (2013) 1013-1024.

[35] A. D. Milov, Y. D. Tsvetkov, M. De Zotti, C. Prinzivalli, B. Biondi, F. Formaggio, C. Toniolo, M. Gobbo, Aggregation modes of the spin mono-labeled tylopeptin B and heptaibin peptaibiotics in frozen solutions of weak polarity as studied by PELDOR spectroscopy, J. Struct. Chem., 54(S1) (2013), S73-S85.

[36] A. Akbarzadeh, R. Rezaei-Sadabady, S. Davaran, S. W. Joo, N. Zarghami, Y. Hanifehpour, M. Samiei, M. Kouhi, K. Nejati-Koshki, Liposome: classification, preparation, and applications, Nanoscale Res. Lett. 8 (2013) 102/1-9.

[37] S.A. Dzuba, D. Marsh, ESEEM of Spin Labels to Study Intermolecular Interactions, Molecular Assembly and Conformation, in: A Specialist Periodic Report, Electron Paramagnetic Resonance, Vol. 24, 102–121 Eds. C. Gilbert, V. Chechik, D.M. Murphy, RSC Publishing (2015).

[38] A.D. Milov, Yu.A. Grishin, S.A. Dzuba, Yu.D. Tsvetkov, Effect of pumping pulse duration on echo signal amplitude in four-pulse PELDOR, Appl. Magn. Reson. 41 (2011) 59-67.

[39] H. J. Steinhoff, N. Radzwill, W. Thevis, V. Lenz, D. Brandenburg, A. Antson, G. Dodson, A. Wollmeri, Determination of interspin distances between spin labels attached to insulin: comparison of electron paramagnetic resonance data with the X-ray structure, Biophys. J. 73 (1997) 3287-3298.

[40] A. D. Milov, A. G. Maryasov, Yu. D. Tsvetkov, Pulsed electron double resonance (PELDOR) and its applications in free-radicals research, Appl. Magn. Reson. 15 (1998) 107-143.

[41] K. M. Salikhov, I. T. Khairuzhdinov, R. B. Zaripov, Three-pulse ELDOR theory revisited, Appl. Magn. Reson. 45 (2014) 573-619.

[42] D. A. Erilov, R. Bartucci, R. Guzzi, A. A. Shubin, A. G. Maryasov, D. Marsh, S. A. Dzuba, L. Sportelli, Water concentration profiles in membranes measured by ESEEM of spin-labeled lipids, J. Phys. Chem. B, 109 (2005) 12003-12013.

[43] A. D. Milov, R. I. Samoilova, A. A. Shubin, Yu. A. Grishin, S. A. Dzuba, ESEEM measurements of local water concentration in D_2O-containing spin-labeled systems, Appl. Magn. Reson. 35 (2008) 73-94.

[44] T. Kaneda, Iso-and anteiso-fatty acids in bacteria: biosynthesis, function, and taxonomic significance, Microbiol. Rev. 55 (1991) 288-302.

[45] (a) M. D. Resh, Palmitoylation of ligands, receptors, and intracellular signaling molecules, Sci. Stke, 359 (2006) re14. (b) M.E. Linder, in: Protein Lipidation, 215-240 (F. Tamanoi and D. Sigman, Eds, Academic Press, 2000, San Diego, CA).

[46] M. D. Resh, Regulation of cellular signalling by fatty acid acylation and prenylation of signal transduction proteins, Cell. Signal. 8 (1996) 403-412.

[47] R. P. Bazinet, S. Layé, Polyunsaturated fatty acids and their metabolites in brain function and disease, Nature Rev. Neurosci. 15 (2014) 771-785.

Figure
Click here to download high resolution image

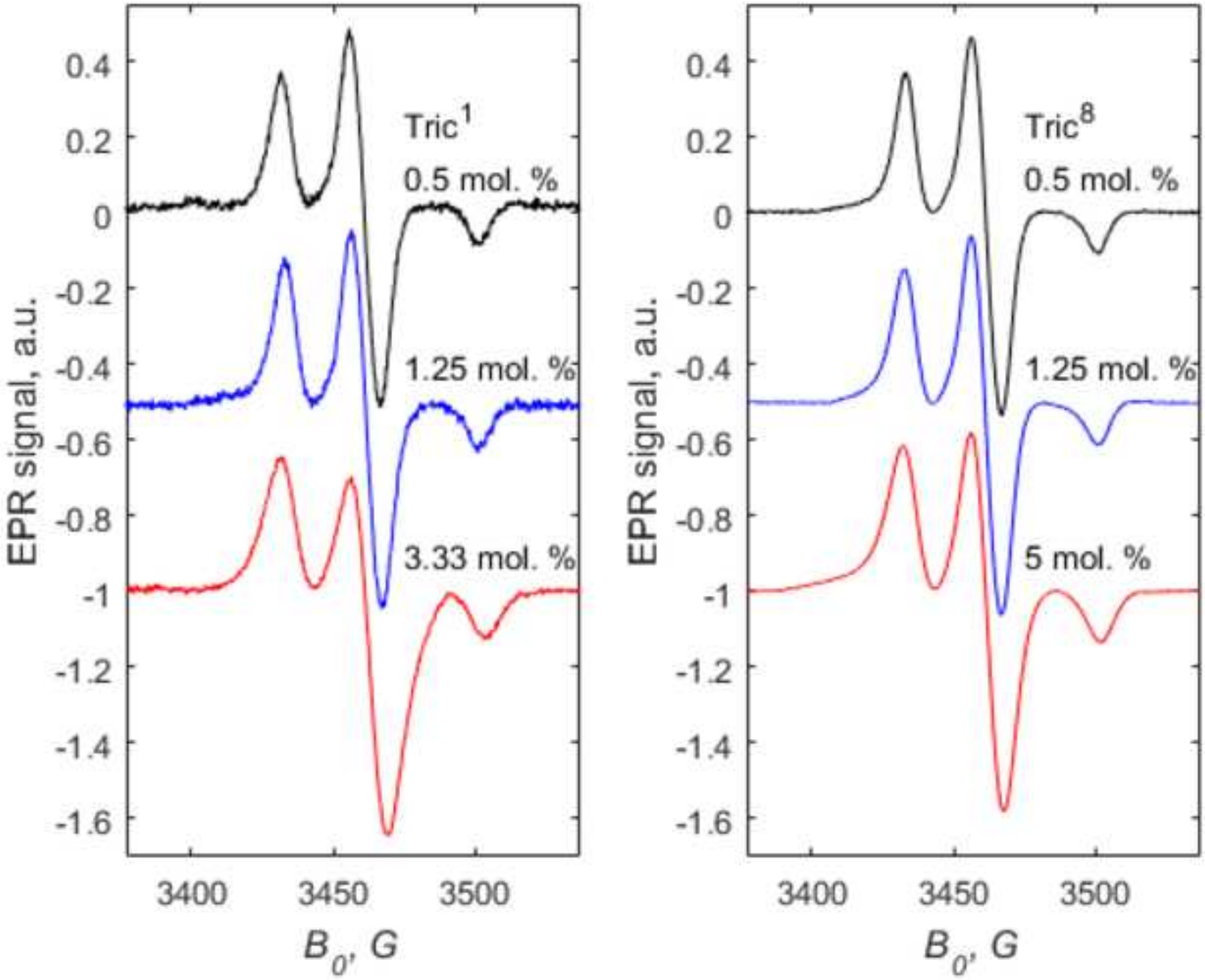

Figure

Click here to download high resolution image

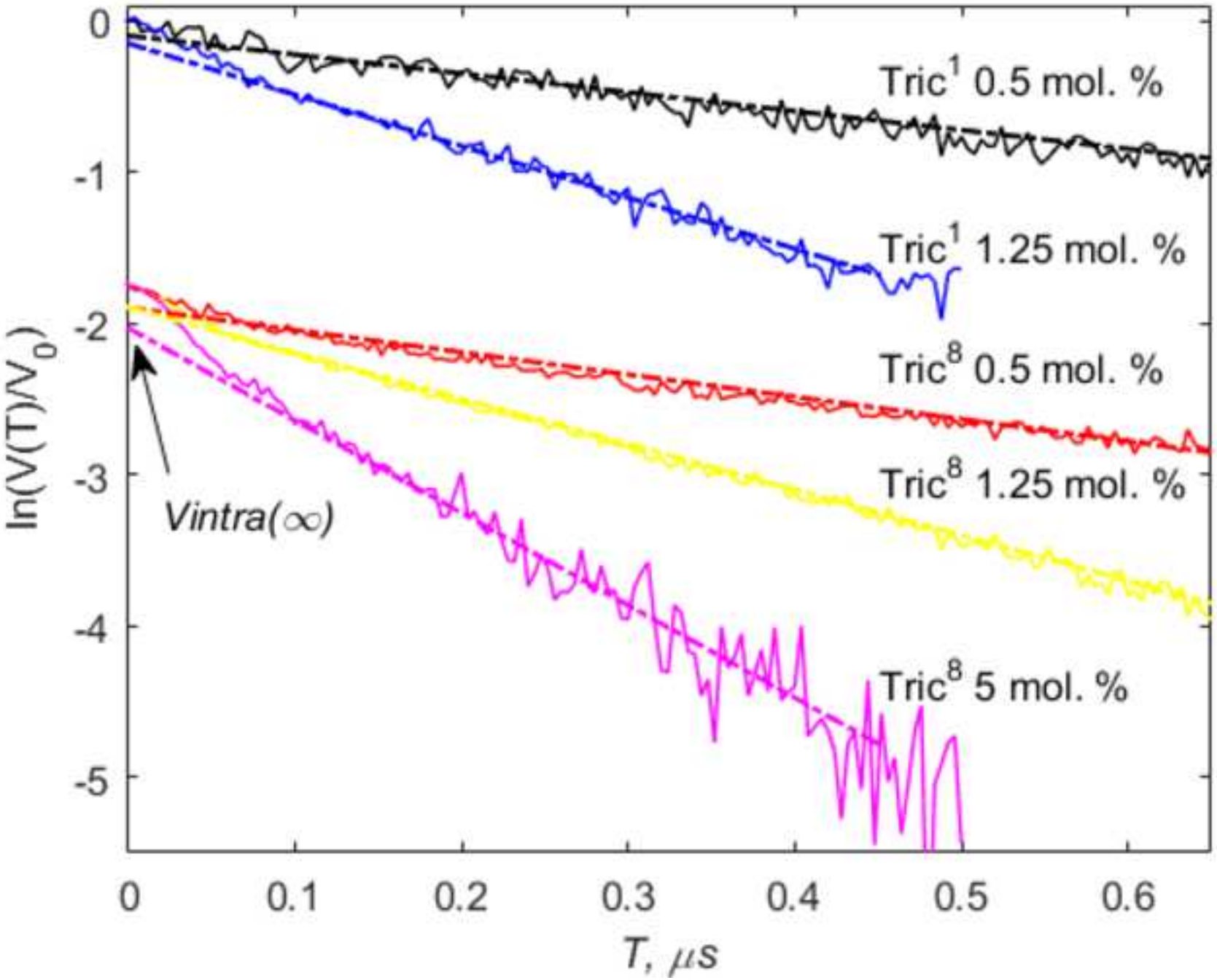

Figure

Click here to download high resolution image

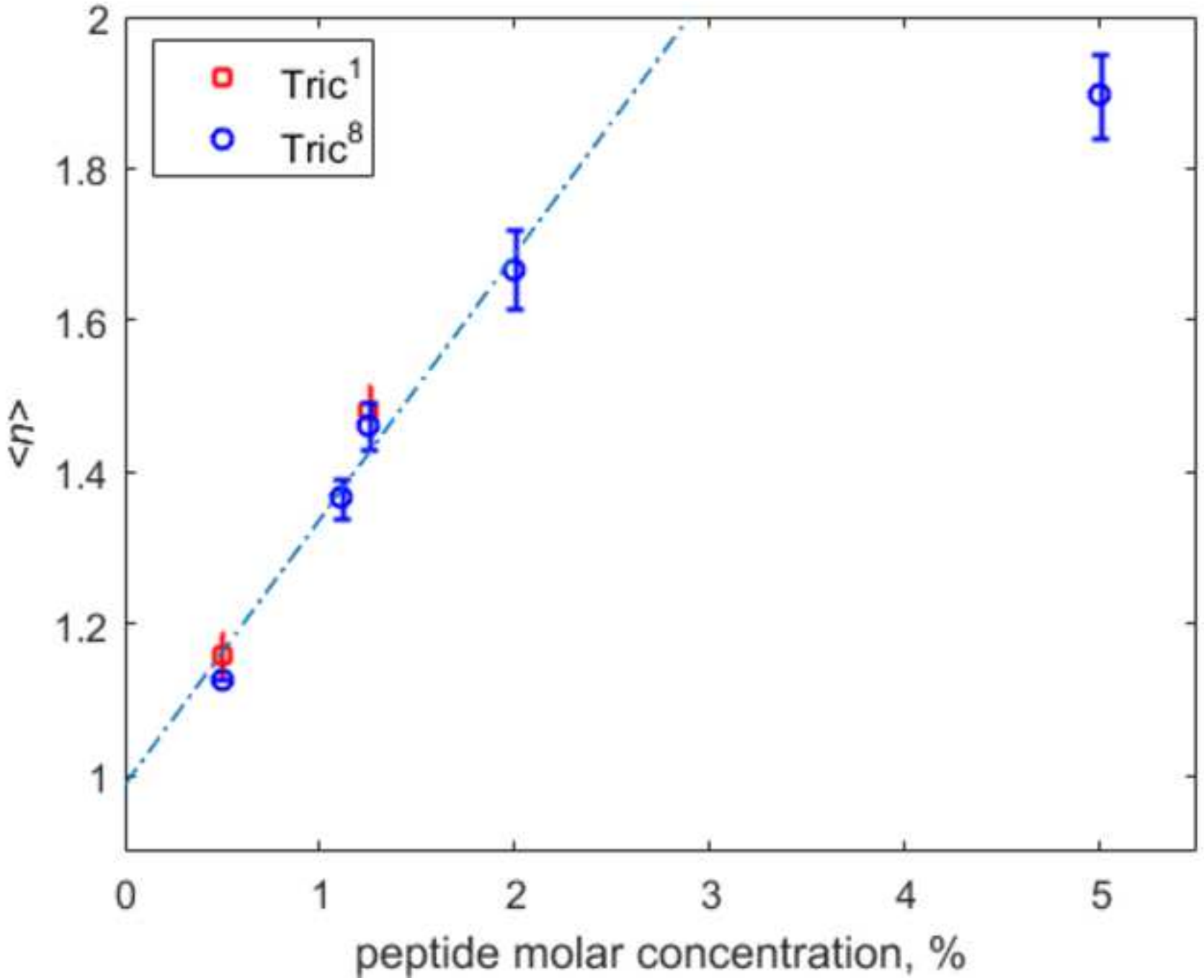

Figure

Click here to download high resolution image

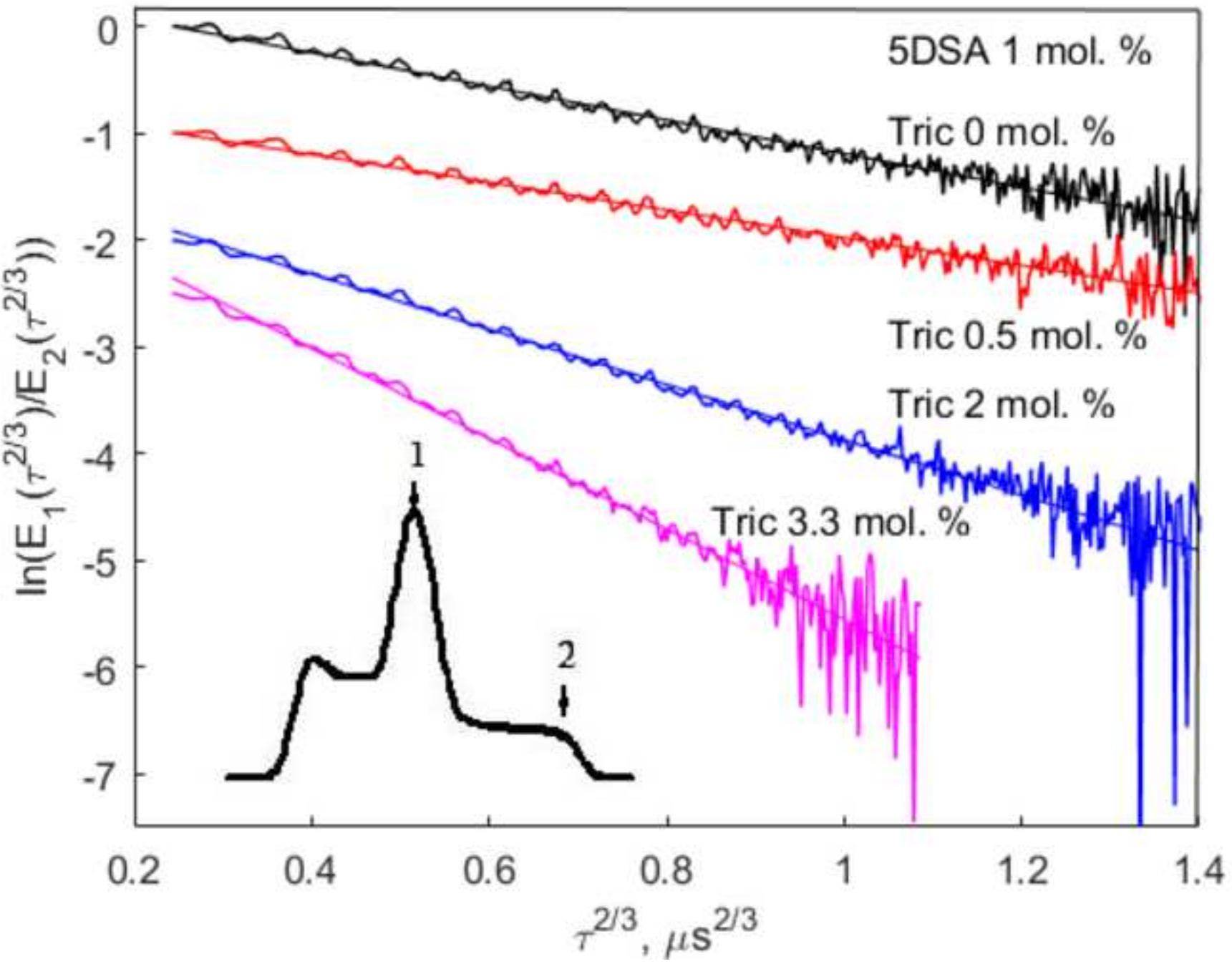

Figure

Click here to download high resolution image

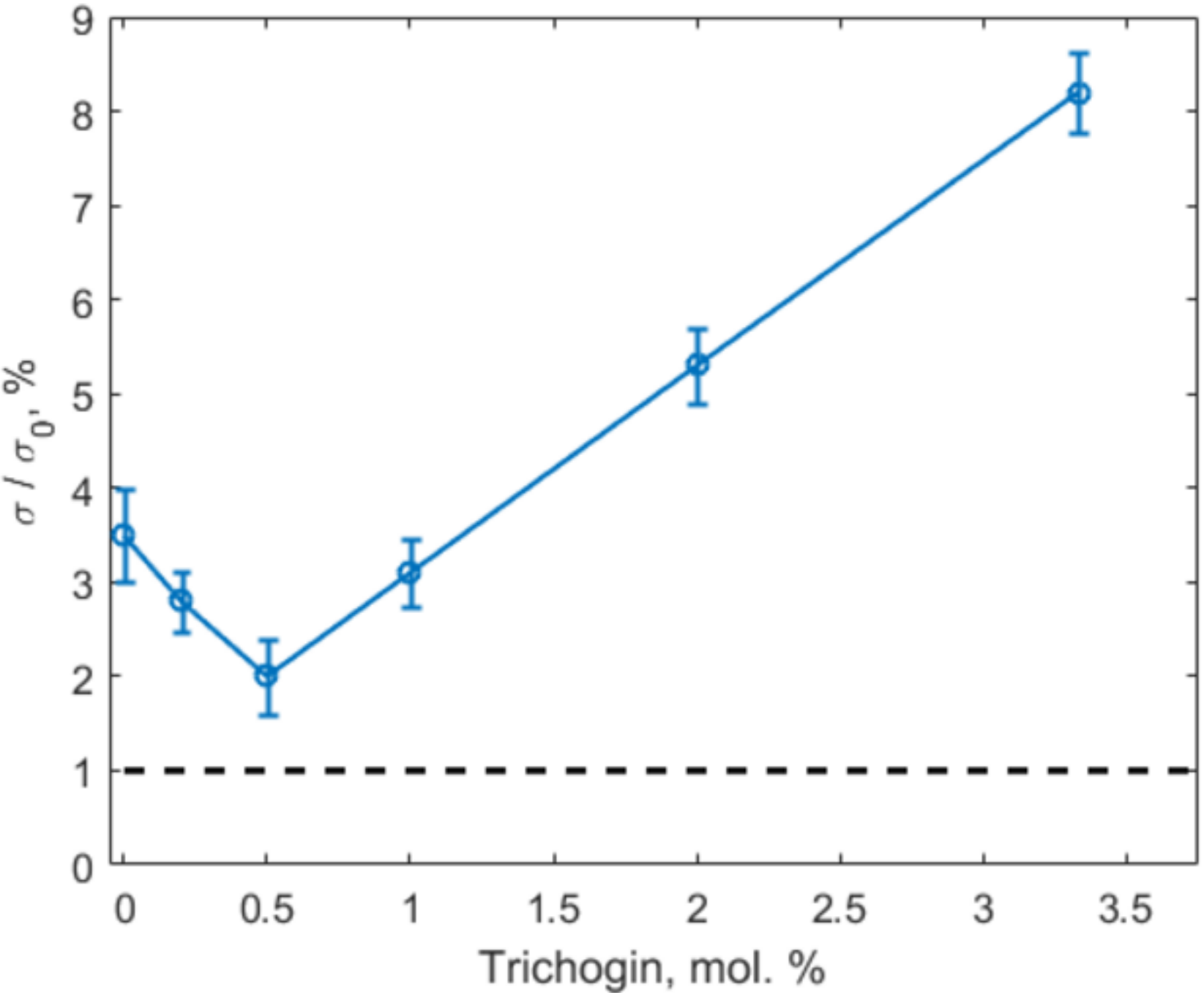

Figure

Click here to download high resolution image

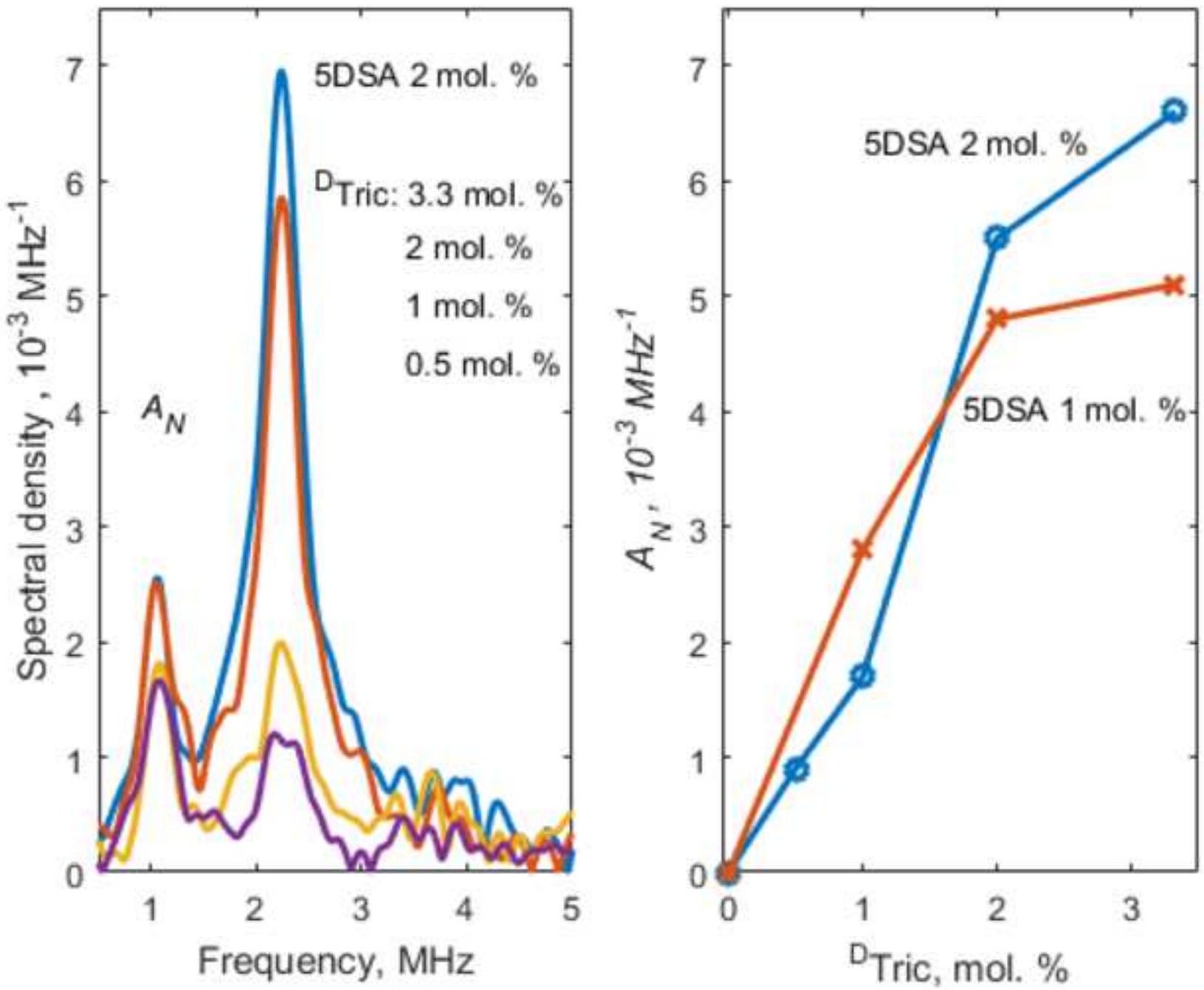

*Conflict of Interest

Institute of Chemical Kinetics and Combustion

Russian Academy of Sciences, Siberian Branch

Ul. Institutskaya-3, Novosibirsk 630090, Russia

Prof. Sergei A. Dzuba
tel: +7 383 3331276
fax: +7 383 3307350
e-mail: dzuba@kinetics.nsc.ru

October 10, 2018

Editorial office

BBA Biomembranes

Dear Editors,

We confirm that in our submitted paper “Peptide antibiotic trichogin in model membranes: self-association and capture of fatty acids” there is no conflict of interests.

On behalf of the authors,

Sergei A.Dzuba